Dynamic polymer hydrogels as synthetic extracellular matrices for 3D cell culture

Liu, T.

CHAPTER 4

Dynamic, cyclic thiosulfinate-crosslinked hydrogels enable cardiomyocyte natural behaviour in 3D

This chapter is prepared as an original research paper: Tingxian Liu, Merel Janssen, Maaike Bril, Roxanne E. Kieltyka*

4.1 Abstract

Dynamic materials have emerged as valuable substrates for a broad range of applications in 3D cell culture because of their viscoelastic properties that closely mimic the *in vivo* cell microenvironment. Disulfide-based crosslinks in covalent polymer materials have shown dynamic character through thiol-disulfide exchange. However, control over their formation in these materials remaining challenging. Herein, we report a strategy for generating disulfide crosslinks in polymer materials in a controlled manner cyclic thiosulfinate-functionalized monomers. Mono-S-oxo-1,2-dithiolane (**ODT**) was reacted with 4-arm polyethylene glycol (PEG) to obtain the hydrogel macromer, **PEG-4ODT**, and subsequently with thiol PEGs to rapidly form hydrogels with dynamic and self-recovering properties. To increase the stability of the formed networks, static thiol/vinyl sulfone crosslinks were introduced into the same hydrogel, while retaining their self-healing character and improving their stablility for long term cell culture (14 days). Additionally, this viscoelastic hydrogel supported the culture of hESC-derived cardiomyocytes in 3D, showing cells with elongated morphologies, spontaneous beating and cell alignment while none of them was observed in static hydrogels. The **ODT** unit was proven to be efficient in rapid hydrogel formation while maintaining the viscoelastic character of the materials. Together with thiol/vinyl sulfone crosslinks, the dynamic hydrogel was validated as an efficient matrix for the long term 3D culture of cardiomyocytes that facilitates their native behavior (*e.g.* alignment, beating) and further underlines the importance of the use of dynamic materials for 3D cell culture applications.

4.2 Introduction

The progress of 3D cell culture models is rapidly advancing research in areas of drug discovery, disease modeling, regenerative medicine and tissue engineering due to their indispensable roles in narrowing the gap between *in vitro* culture and *in vivo* conditions.[1–3] The abundant choice in cell source offers the possibility to develop a wide range of models that can mimic healthy and diseased states of tissues. Induced pluripotent stem cells stand out in this regard because of their capacity to differentiate into virtually any cell type of the human body while retaining genetic features of the patient they are obtained from, providing a personalized view in the above areas. In the field of drug discovery there is an interest to develop improved cellular models to better predict toxicity of therapeutic candidates. However, cardiomyocytes derived from induced pluripotent stem cells show distinct morphological, electrical and functional properties in comparison to their adult counterparts because of their fetal-like character.[4–6] These immature features limit their ability to accurately predict patient responses, but further underscore the need to better understand the conditions necessary to promote their maturity.

Natural materials, such as Matrigel, gelatin and collagen, have been widely explored to support the growth cells and tissues. Although they provide numerous biological cues, these matrices are chemically undefined and lack the potential to tune their mechanical properties to match a variety of tissues.[7–10] In contrast, synthetic polymer hydrogels provide an alternative water-rich platform that is chemically defined, with tunable mechanics that can approximate the stiffnesses of a range of tissues.[11–13] In these materials static crosslinks efficiently maintain the gel state during culture, however the materials lack the ability to recapitulate viscoelasticity of native tissues affecting parameters such as cell migration that is critical for morphogenesis.[14] Thus,

synthetic polymer materials that can achieve the stiffness of adult tissues, but contain viscoelastic properties are necessary to support cell behavior in complex processes such as those that are found in development to further refine the available cell culture models.

Dynamic covalent bonds that combine strength of static covalent bonds and reversibility of non-covalent interactions have been broadly applied in the field of polymer chemistry to engineer the viscoelasticity of covalent polymer materials.[15–18] Boronates,[19] disulfides,[20] Diels–Alder adducts,[21,22] thioesters,[16,23] Schiff bases,[24] aldehydes and hydrazides have been frequently reported in this line.[25,26] However, the use of these bonds as crosslinks on their on can be insufficient with respect to machanics and stability in applications such as 3D cell culture. Thus, their combination with static covalent bonds has been examined as a strategy to further control these features for applications in tissue culture. The obtained network benefits from the synergy in properties between both crosslinks, *e.g.* physical and reversible crosslinks that are dynamic and self-healable, and static covalent crosslinks that provide mechanical stiffness and stability.[27–31] For example, Anseth and co-workers employed the boronate chemistry to fabricate an adaptable PEG hydrogel, in which the cis-1,2-diols are crosslinked with boronic acids resulting in a dynamic hydrogel displaying a fast stress relaxation profile. A secondary static crosslink is required support a stable 3D cell culture platform in presence of serum containing media.[19]

Among the dynamic covalent bonds, disulfide chemistry is attractive for biomaterials applications because of its biological relevance and reversibility under mild conditions with respect to various stimuli (*e.g.* redox, light, heat). However, the introduction of crosslinks based on disulfides can sometimes prove challenging due to premature cross-linking of the polymers prior to their application. Hence, latent or protecting group strategies have been used to facilitate their introduction into polymer materials. Latent strategies using cyclic 1,2-dichalcogenides, such as 1,2-dithiolanes,

are attractive because of their capacity to form poly(disulfides) on ring opening polymerization through the addition of nucleophiles or light in water. Moreover, thiol/cyclic 1,2-dithiolane exchange reactions were faster than that of thiol and linear disulfide,[32,33] and these reactions are reversible and tunable, depending on the substituent pattern on the cyclic dithiolane ring.[34] Waymouth and co-workers designed novel water-soluble triblock (ABA) copolymers with pendant 1,2-dithiolanes that form hydrogels based on thiol-initiated ring opening polymerization of pendant 1,2-dithiolanes with shear-thinning and dynamic flow behaviors as a result of the formed disulfide polymers.[20,35] Recently, we reported use of cyclic 1,2-dithiolanes to crosslink with norbornene on linear PEG polymers through UV irradiation obtaining hydrogel materials with branched macromolecular architectures and self-recovering properties.[36] However, due to the use of small molecules or light to facilitate their crosslinking, their application can be challenging when more sensitive cell types are involved and thus, latent strategies that enable gel formation in a controlled and rapid manner with high cytocompatibility remain necessary.

Thiosulfinates are intermediates obtained in the oxidation of thiols to sulfonic acids. While efficient in making disulfide-containing compounds, in most cases, the linear thiolsulfinates easily decompose upon heating. Recently, Donnelly *et al.* reported several chemically stable cyclic thiosulfinates that were easily synthesized by oxidication of cyclic disulfide. The use of cyclic thiosulfinates for protein crosslinking was validated, reacting rapidly (~10 min, >95% conversion) in comparison to days in the case of 1,2-dithiane.[37] Because of the rapid protein cross-linking kinetics, we became interested in the capacity of this latent thiol strategy to crosslink polymer materials for 3D cell culture applications. We introduced 1,2-dithiolane-1-oxide (**ODT**) on a 4-arm PEG macromer (**PEG-4ODT**) and evaluated its triggering by thiol-functionalized PEG (**PEG-4SH**) to form polymer materials with disulfide crosslinks. We further examined the use of this cross-linking chemistry to prepare scaffolds with modular stiffness for

the 3D culture of embryonic pluripotent stem cell derived cardiomyocytes focusing on understanding the consequence of their dynamic character driving native cell behaviours.

4.3 Results and Discussion

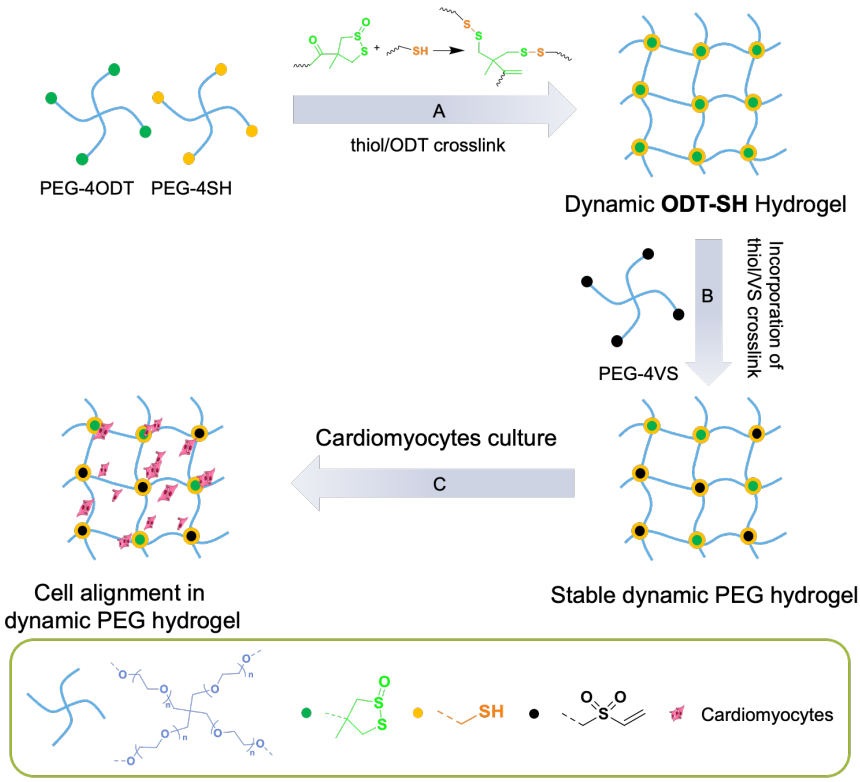

Scheme 4.1. A) Preparation of dynamic ODT-SH hydrogels: mixing of PEG macromers **PEG-4ODT** and **PEG-4SH** yields dynamic disulfide crosslinked hydrogels with tunable stiffnesses. B) After incorporation of thiol/VS crosslinks by mixing of **PEG-4VS** macromers, a stable and dynamic PEG hydrogel was obtained. C) Cardiomyocytes that were 3D cultured in this dynamic PEG hydrogel displayed natural cell behavior: cell alignment.

ODT-crosslinked hydrogel preparation and characterization. Two PEG macromers, end-functionalized with a cyclic disulfide (dithiolane, **DT**), and a cyclic thiosulfinate

(**ODT**) were first synthesized (Scheme S4.1). **DT** and **ODT** with carboxylic acid handles were synthesized according to previous reports,[38] prior to coupling coupled onto hydroxy PEG macromers through Steglich esterification in presence of N,N'-dicyclohexylcarbodiimide (DCC) and 4-dimethylaminopyridine (DMAP). The **DT** (**PEG-4DT**) and **ODT**-functionalized 4-arm PEG macromers (**PEG-4ODT**) were obtained by precipitation in cold diethyl ether and dialyzed against water with a high degree of end-functionalization (**PEG-4DT** ca. 86%, Figure A4.5; **PEG-4ODT** ca. 90%, Figure A4.6). Following a similar protocol, the **ODT**-functionalized linear PEG macromer (**PEGdiODT**) was prepared with a high degree of functionalization of 86%. Detailed synthetic information can be found in the Supporting Information.

To prepare the hydrogels, stock solutions of PEG macromers **PEG-4DT** and **PEG-4ODT** were first dissolved in PBS (pH 7.4) and mixed in particular ratios to result in their gelation. Gel inversion tests were first performed on hydrogels consisting of **PEG-4ODT** and **PEG-4SH** (**ODT-SH** hydrogels) at a fixed thiol/ODT molar ratio to gain insight into the concentrations where gels are formed and gelation time. Transparent hydrogels were formed when the total PEG macromer concentrations were higher than 4 mM with thiol/ODT molar ratios at 1:1 and 2:1 (Figure S4.1 and S4.2), while no hydrogels were formed using the same conditions for **PEG-4DT** and **PEG-4SH**. This result points to the decreased reactivity of thiol/DT pair in comparison thiol/ODT pair, and is consistent with an earlier report of Agar and co-workers.[37] Notably, **ODT-SH** hydrogels formed within 5 min when the PEG macromer concentration was higher than 6 mM, showcasing the rapid kinetics of the thiol/ODT reaction and suitability for 3D cell culture applications. Moreover, the gelation kinetics were faster than the thiol/VS bioconjugation reaction where 10 mins were necessary to form hydrogels on a PEG macromer concentration of 12 mM (Figure S4.3). To better understand the thiol/ODT reaction on polymer materials, linear PEG macromers with **ODT** were also prepared. Hydrogels were formed at a total PEG macromer concentration of 10 mM suggesting

the reaction of one **ODT** moiety with more than one thiol group to form a crosslinked network between linear PEGs. This rapid crosslinking between thiol and **ODT** opens a new route to prepare hydrogels from both star and linear PEG macromers under cell culture conditions.

Oscillatory rheology measurements were performed to quantitatively assess the gelation time and mechanical properties of the disulfide networks. The **ODT-SH** hydrogels showed storage moduli (G') that were significantly greater than the loss moduli (G'') with tunable stiffness and gelation time based on macromer concentration. In contrast, the mixing of **PEG-4DT** and **PEG-4SH** resulted in a rheological profile consistent with the lack of gel formation (G''>G') (Figure 4.1A). The stiffness of **ODT-SH** hydrogels can be tuned from 200 Pa to 5 kPa by varying total PEG macromer concentration from 4.5 to 8 mM. Moreover, the gelation time also decreased from 10 to less than 1 min with increasing the total PEG macromer concentration (Figure 4.1B). For **ODT-SH** hydrogel consisting of 3.0 mM **PEG-4ODT** and 3.0 mM **PEG-4SH**, the linear viscoelastic (LVE) region showed a limit of applied strain of 322%. Frequency sweep measurements demonstrated that G' was greater than G'' by two orders of magnitude over the frequency range from 0.01 Hz to 10 Hz, confirming the formation of viscoelastic materials (Figure S4.6). To probe the contribution of the dynamic thiol/ODT crosslinks to the **ODT-SH** hydrogel mechanical properties, we tested their capacity to self-recover by performing a step-strain experiment. The storage modulus (G') recovered more than 90% of its original value after the application of large strain (700 %) within 2 min (Figure 4.1C). Alternating the strain from high (700%) to low (0.05%) in a cyclic manner further exposed the potential recovery property of the materials. Considering their subsequent application as 3D cell culture materials, the mechanical properties of the hydrogels were further tested at 37˚C. The data showed that G' measured at room temperature was 5.4, 3.5, 2.2 and 1.9 times higher than the samples measured at 37˚C when total PEG macromer concentrations were 4.5, 5, 6,

and 8 mM, respectively (Figure 4.1D). The decreased stiffness of the materials likely results from the increased rate of thiol/disulfide exchange at 37˚C,[39] further indicating the formation of disulfide crosslinks and the inherent dynamic character of the network. Importantly, the **ODT-SH** hydrogel retained its viscoelastic and self-healing properties at 37˚C, opening the door to its future use in 3D cell culture applications (Figure S4.7).

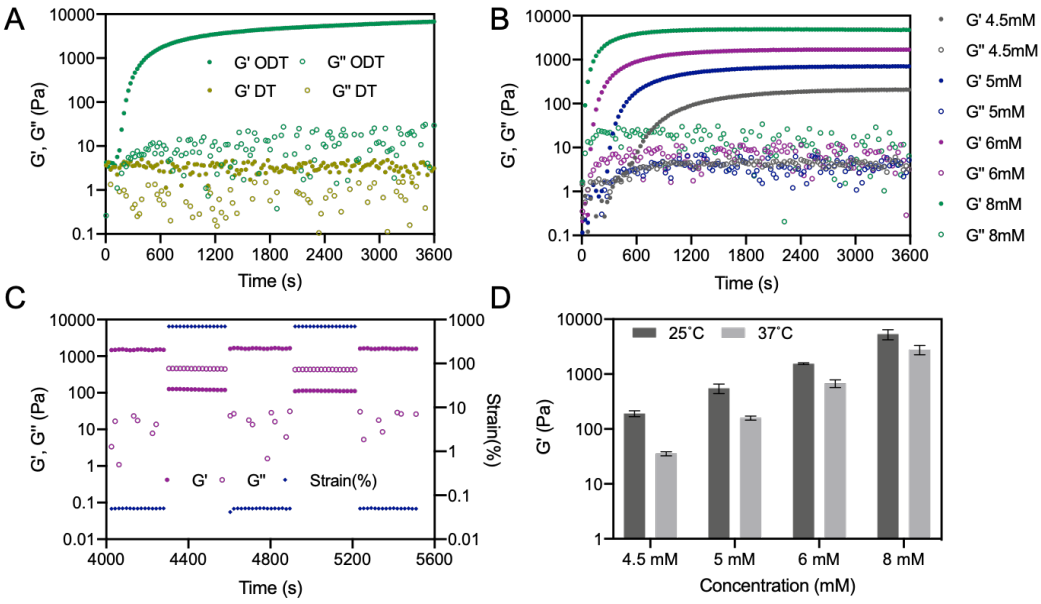

Figure 4.1. A) Storage (G') and loss moduli (G'') of **ODT-SH** hydrogels and **DT-SH** networks collected by a time sweep measurement at 25 ± 0.2˚C with a fixed frequency of 1 Hz and strain of 0.05%. B) Time sweep measurements of **ODT-SH** hydrogels with total PEG macromer concentrations of 4.5, 5, 6 and 8 mM. G' and G'' were collected at 25 ± 0.2˚C with a fixed frequency of 1 Hz and strain of 0.05% until a plateau in the moduli was obtained. C) Step-strain measurements of **ODT-SH** hydrogel (6 mM) at 25 ± 0.2˚C with a frequency of 1 Hz; Low (0.05%) and high strain (700%) were applied for 300s alternatively for two times. D) Averaged storage moduli (G') of **ODT-SH** hydrogels that measured under 25 ± 0.2˚C and 37 ± 0.2˚C with total PEG macromer concentrations at 4.5, 5, 6 and 8 mM, respectively. (N = 3)

To characterize crosslinking of thiol/ODT at molecular level, nuclear magnetic resonance (NMR) and liquid chromatography–mass spectrometry (LCMS) experiments were performed using model molecules. The reaction between **ODT** unit and glutathione (GSH) in deuterated water (D_2O) was monitored by NMR spectroscopy, and changes to **ODT** were followed tracking the chemical shift of the -CH_3 group. Unreacted **ODT** shows a chemical shift of 1.62 ppm for the -CH_3 group, whereas its reaction with GSH shows an upfield shift 1.48 ppm to 1.31 ppm. After 75 h incubation using a thiol/ODT molar ratio of 1:1, 51% ODT was consumed and this value increased to 100% when the thiol/ODT molar ratio was increased to 2:1, 4:1 and 8:1, implying that **ODT** reacts with GSH in a 1:2 molar ratio. Moreover, LCMS data supports the determined ratios from NMR, as **ODT** molecules were transferred into compound **M1** (t=2.55 min, m/z 777.25), as previously reported for the crosslinking of proteins with cyclic thiosulfinate. When **ODT** was treated with excess GSH (thiol/ODT molar ratio at 4:1 and 8:1), a major shift from 1.31 to 1.48 ppm was recorded and a new compound **M3** (t=3.17, m/z 942.67) was identified. These results indicate that the thiol/ODT crosslinking reaction involves two steps: one, the **ODT** reacts with GSH in a molar ratio of 1:2; two, **M1** undergoes further thiol/disulfide exchange in presence of thiols to form product **M3** (Figure S4.5).

To investigate the applicability of the thiol/ODT chemistry for 3D cell culture, NIH 3T3 cells were encapsulated within the **ODT-SH** hydrogels. PEG macromer concentrations were kept at 6 mM and thiol/ODT molar ratios were varied from 1:1, 2:1 and 4:1 (Figure S4.10). From LIVE/DEAD staining results, over 95% cells remained viable after 2 h culture and were homogeneously distributed throughout the gel. After 48 h cell culture, while the cells maintained high viability (> 80%) they settled down to the bottom due to the dissolution of hydrogel over the culture period. This result is likely due to the dynamic character of the polymer materials due to the disulfide

crosslinks, as similar behavior has been reported for other dynamic hydrogels.[19,40] Thus, to overcome the rapid gel erosion encountered in the **ODT-SH** hydrogels under the cell culture conditions, static thiol/VS crosslinks based on permanent covalent bonds were introduced into the polymer networks at the expense of the thiol/ODT crosslinks.

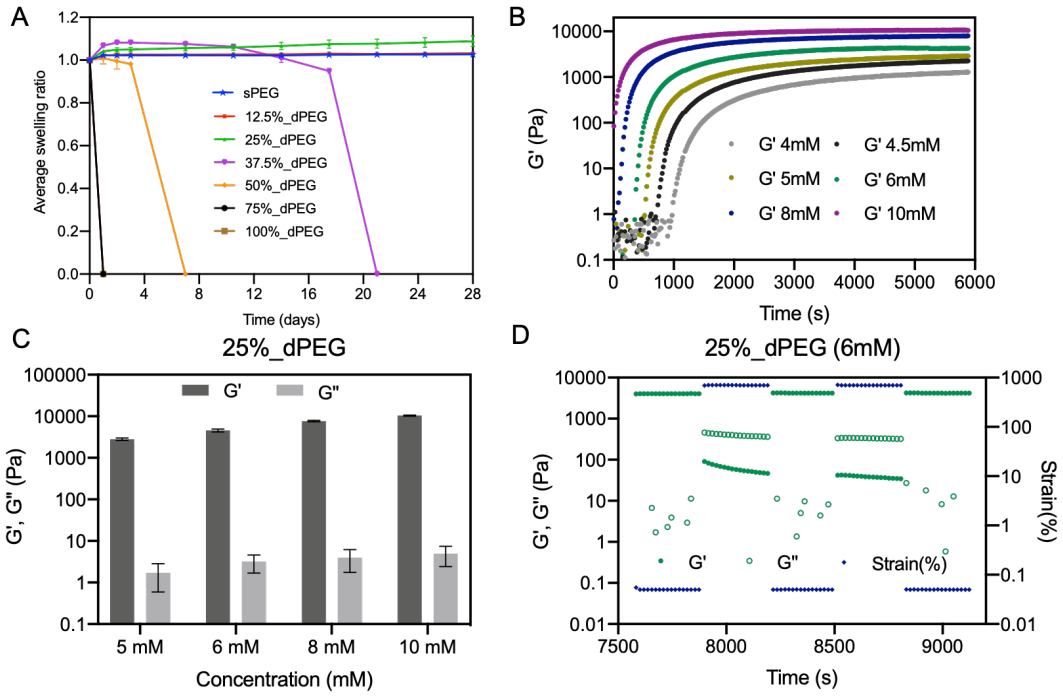

Figure 4.2. Characterization of dynamic PEG hydrogels that consist of both dynamic and static crosslinks. A) Swelling measurements of PEG hydrogels: swelling ratios were examined as a function of the percentage of dynamic disulfide crosslinks on a total PEG macromer concentration of 6 mM. B) Oscillatory rheology time sweep measurements of **25%_dPEG** hydrogels at total PEG macromer concentrations of 4, 4.5, 5, 6, 8 and 10 mM. Storage (G') and loss moduli (G'') were collected at 37 ± 0.2˚C with a fixed frequency of 1 Hz and strain of 0.05% until a plateau in the moduli was reached. C) Averaged (N = 3) plateau moduli, G' and G'', of **25%_dPEG** hydrogels at total PEG macromer concentrations of 5, 6, 8 and 10 mM from frequency sweep measurements.

D) Step-strain measurements of **25%_dPEG** (6 mM) at 37 ± 0.2˚C at a frequency of 1 Hz; low (0.05%) and high strain (700%) were applied in alternation for 300s over two cycles.

Dynamic PEG hydrogel preparation and characterization. Hydrogels prepared from exclusively thiol/VS crosslinks are known to be stable and support cell culture in presence of medium containing serum.[41] Therefore, swelling experiments were performed on gels with both static and dynamic covalent crosslinks to determine the ratio of dynamic and static bonds necessary to prepare gels stable for cell culture experiments. Hydrogels with 12.5%-100% thiol/ODT crosslinks were prepared keeping the total PEG macromer concentration at 6 mM, and then incubated with cell culture medium at 37˚C. As observed in earlier viability experiments, **ODT-SH** hydrogels that consist of exclusively thiol/ODT crosslinks were completely dissolved within 24 h. In contrast, hydrogels formed from 100% thiol/VS crosslinks (**sPEG**) remain stable over the entire duration of the experiment (28 days) (Figure 4.2A). However, hydrogels containing 25% or less thiol/ODT crosslinks showed comparable stability to the **sPEG** hydrogel over a 28-day period. Based on their stability under cell culture conditions, the **25%_dPEG** network was selected for further culture experiments.

The consequence of including permanent cross-links on the mechanical properties of the **25%_dPEG** network was further examined using oscillatory rheology. Similar trends were observed to the **ODT-SH** hydrogels in the various experiments. The stiffness of **25%_dPEG** hydrogels displayed a concentration-dependent trend, in which G’ varied from 1.3 kPa to 10.4 kPa with varying the total PEG macromer concentrations from 4 to 10 mM. The gelation time decreased with increasing PEG macromer concentration from 16 min to less than 1 min (Figure 4.2B and 4.2C). The LVE region was determined by performing an amplitude sweep experiment in a range of strain from 0.1% to 1000% and a fixed frequency of 1 Hz. In the case of **25%_dPEG** hydrogels (5 mM and 6 mM), G’ and G’’ remained constant until 56% strain, whereas for

25%_dPEG hydrogels (8 mM and 10 mM) a shift from the linear regime was observed at a strain of 99%. During frequency sweep measurements ranging from 0.01 Hz to 10 Hz, in all test concentrations, G' was greater than G'' by two orders of magnitude confirming the formation of viscoelastic materials from hybrid crosslinks (Figure S4.8). Most importantly, a high self-recovery capacity (~90%) was observed in all **25%_dPEG** hydrogels after applying high strain (700%) and low strain (0.05%) alternatively for two cycles (Figure 4.2D and S4.9). Overall, the combination of the long-term stability and high self-recovery capacity of the covalent networks with 25% dynamic thiol/ODT crosslinks can be useful for healthcare applications.

As a first approach to cell culture within **25%_dPEG** hydrogel**,** cell encapsulation and viability experiments were performed. NIH 3T3 cells were encapsulated in 3D within **25%_dPEG** hydrogels using total PEG macromer concentrations of 4.5, 6 and 10 mM and cultured for 4 days. LIVE/DEAD staining of the hydrogels after this time period showed that the cells were mainly green-stained for all tested conditions indicating that the **25%_dPEG** hydrogel is cytocompatible (Figure 4.3). It should be noted that a lot of cells settled down in case of 6 mM hydrogels after 4 days of culture. Since the swelling ratio of **25%_dPEG** hydrogel at this concentration stays stable at 1.06, we infer that there is an interaction between dynamic hydrogels and cellular thiols or disulfides that results in the dissolution of network leading to cell sedimentation. Even though cell sedimentation occurred gradually after 4 days of culture, the **25%_dPEG** hydrogel still supported cells within the well. When a higher concentration of PEG macromers of **25%_dPEG** hydrogel was used (10 mM), cells were supported in 3D with a reasonable cell viability (>60%) during the 4 days of culture, after which cell-laden hydrogel can be easily taken up by a spatula. Taken together, **25%_dPEG** hydrogel was proven to be cell compatible at both low (4.5 mM) and high (10 mM) PEG macromer concentrations and long-term culture can be realized by introducing the second thiol/VS crosslink into 100% thiol/ODT hydrogels.

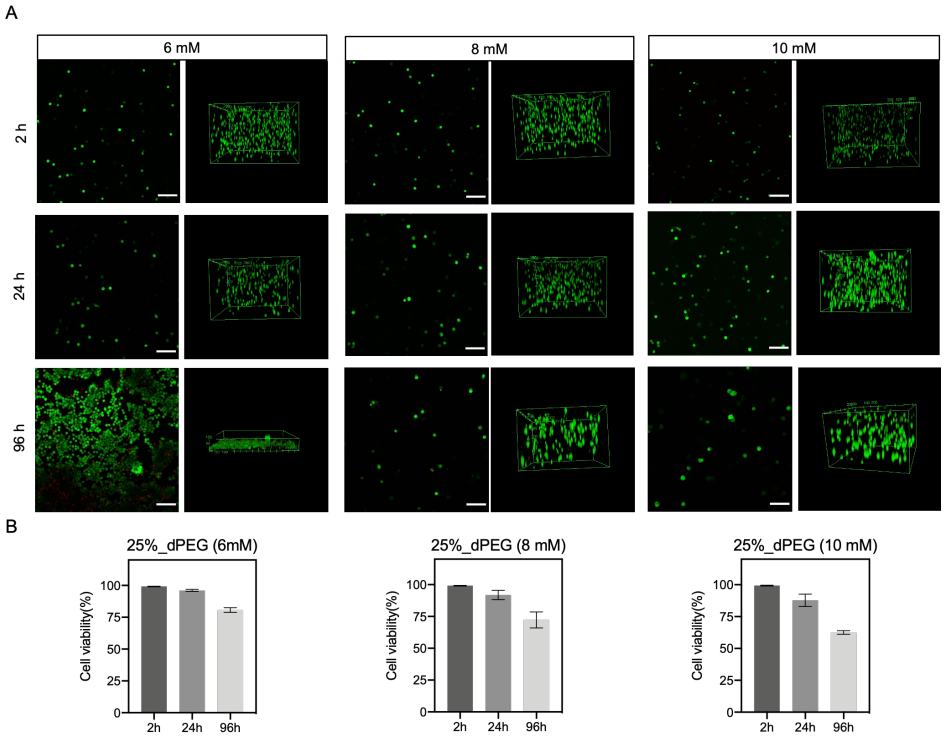

Figure 4.3. 3D cell culture in **25%_dPEG** hydrogels with total PEG macromer concentrations of 6, 8 and 10 mM. A) Representative 2D images and z-stack 3D overview of cells in **25%_dPEG** hydrogel (6 mM) after 2, 24 and 96h culture. Cells were stained with calcein AM (viable cells, *green*) and propidium iodide (PI) (dead cells, *red*). Scale bar = 100 µm. B) Cell viability percentages were calculated by cell counting in Fiji after LIVE/DEAD staining. The means and standard deviations are marked inside the graphs, N=3.

Maturation of hESC-derived CMs within 25%_dPEG hydrogel. The matrix microenvironment plays an important role in guiding cell behavior, for example, the morphology, spontaneous contraction and eventually, maturation of CMs. Few examples have been reported in fabricating dynamic materials while decoupling the biological cues to understand their effect on cell fate. In this work, a genetically modified hESC cell line was used that shows fluorescence through GFP for the cardiac transcription marker Nkx2.5 and mRuby for α-actinin. First, the hESC-derived CMs were

prepared by seeding hESCs on Matrigel coated plates and differentiated as a monolayer using the STEMdiff™ Cardiomyocyte Differentiation Kit. Bright field and fluorescence microscopy images of their differentiation in 2D were taken over a 28-day period as a control. As shown in Figure S4.11, the hESCs started to express the cardiac transcription factor Nkx2.5 (GFP fluorescence) on day 7, and the expression became more uniform across the cells during their further differentiation. Conversely, expression of α-actinin as observed from the fluorescence of mRuby is hardly visible until day 9, increasing in intensity after day 14 and maintained a uniform expression until day 28. Notably, sarcomeres were visualized through the mRuby labeled α-actinin showing mainly disordered structure that does not resemble the organization of sarcomeric α- actinin in native human myocardium.[42] RT-PCR experiments were subsequently performed to obatin a quantitative insight into cardiac and pluripotent gene expression. As seen in Figure S4.12, expression of pluripotent genes Oct4, Sox2 and Nanog was significantly decreased over the differentiation period ($P<0.0001$). Meanwhile, increased expression of cardiac structural genes cTnT, MYH6 and MYH7 were measured that is in line with the experimental observation of spontaneously beating cardiomyocytes in the culture. Cx43 protein that codes for gap junctions that are critical for synchronous contraction of CMs, showed significantly decreased expression after 8 days of differentiation ($P<0.01$) and remained low during the whole differentiation process supporting the inhomogeneous beating of cardiomyocytes. Taken together, the increased expression of cardiac makers and genes together with significantly decreased pluripotency gene expression demonstrated the successful differentiation of the hESC reporter line to cardiomyocytes in 2D.

The hESC-CMs were collected after being prepared as a monolayer and reseeded in 3D in the **25%_dPEG** and **sPEG** hydrogels to study their cell behavior in 3D with respect to various stiffnesses. From the confocal microscopy images, hESC-CMs cultured within all tested hydrogels maintained the expression of Nkx2.5_GFP and the

α-actinin_mRuby (Figure 4.4). Spontaneous beating was not immediately observed after seeding in 3D, but after 3 days of culture, hESC-CMs encapsulated in **25%_dPEG** (6 mM, 4.5 kPa) hydrogel started beating, becoming more robust with further culture. The loss and recovery of spontaneous beating of CMs is on par with literature reports that show 2-3 days are necessary to regain this behavior.[43,44] In case of **sPEG** hydrogel, hESC-CMs did not spontaneously beat after reseeding, and even after further culture pointing out the importance of a dynamic environment to promote native hESC-CM behavior. Recovery of the beating of hESC-CMs was observed on day 14 for **25%_dPEG** hydrogels with higher concentration and stiffness (8 mM, 8 kPa), whereas further increasing the stiffness did not yield any cell beating in **25%_dPEG** hydrogels (10 mM, 10.5 kPa). This observation can be rationalized by the inverse correlation between substrate stiffness and CM contraction,[45] that is, increased stiffness is expected to delay the recovery of hESC-CM contraction.

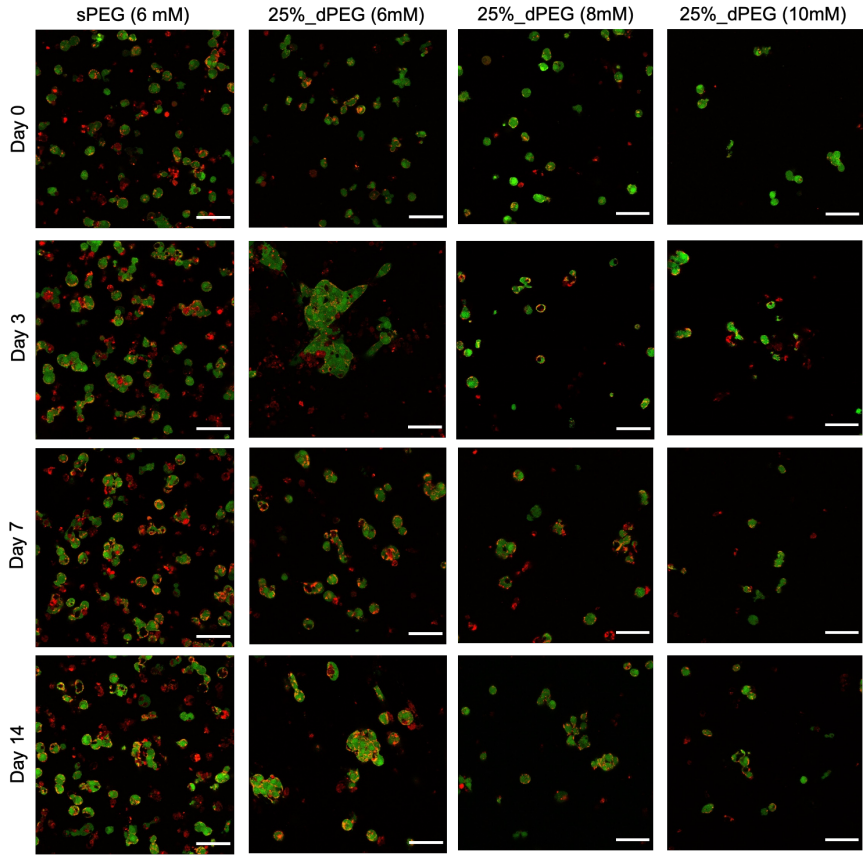

Figure 4.4. Representative confocal microscopy images of hESC-CMs reseeded and cultured within **25%_dPEG** and **sPEG** hydrogels for 14 days after differentiation on Matrigel. Merged flurescent images of cardiac transcription factor Nkx2.5_GFP (Green) and the sarcomeric protein α-actinin_mRuby (Red) of the hESC-CMs after 0, 3, 7 and 14 days of reseeding, respectively. Scale bar: 50 µm.

Morphology of hESC-CMs within the **25%dPEG** and **sPEG** hydrogel were captured by brightfield microscopy using a 10x objective (Figure 4.5). In comparison to the round morphology of hESC-CMs in **sPEG** hydrogel, hESC-CMs cultured in **25%_dPEG** (6 mM) hydrogel displayed an elongated shape. More interestingly, after one day of culture, hESC-CMs started to spontaneously align in this soft and dynamic hydrogel (G' 4.5 kPa), behaving similarly to the alignment of CMs in native tissues. Also, hESC-CMs started to show a similar alignment in the **25%_dPEG** hydrogel (8 mM) on day 14. In case of stiff

25%_dPEG hydrogel (10 mM), cells displayed a round morphology and no alignment were observed over the culture period. This trend in cell behavior in **25%_dPEG** hydrogel with respect to the beating of hESC-CMs, therefore, it is likely the dynamic nature of the hydrogel plays critical role in supporting their native behaviors.

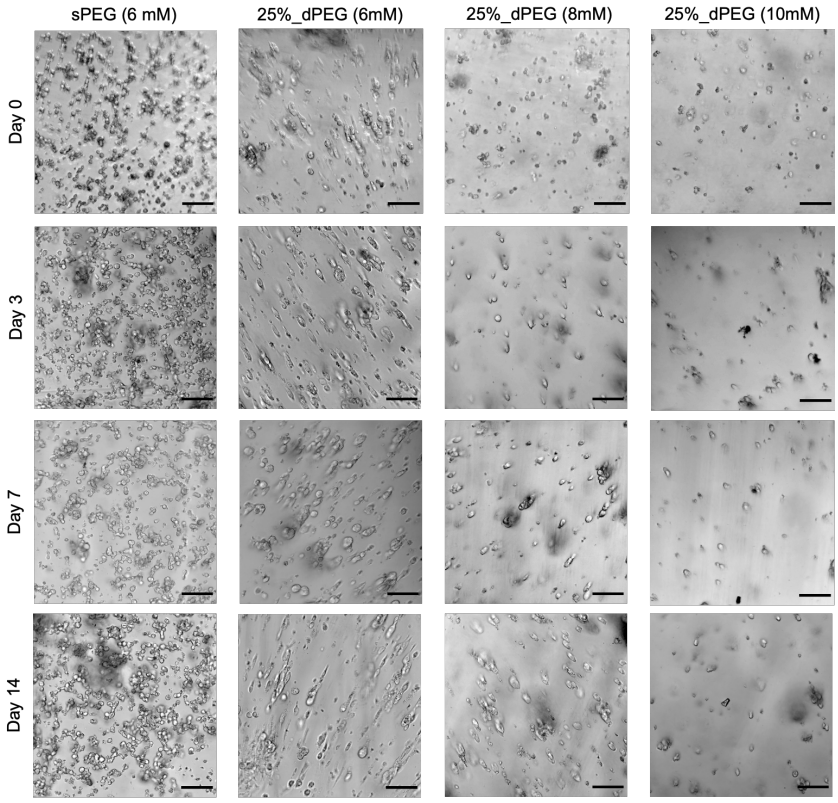

Figure 4.5. Bright field microscopy images of hESC-CMs that differentiated in 2D for 14 days and then cultured in **25%_dPEG** (6, 8, 10 mM) and **sPEG** (6 mM) hydorgels for 3, 7 and 14 days, respectively. Scale bar: 100 µm.

To gain more quantitative information about cardiomyocyte maturation in the dynamic hydrogels in 3D, RT-PCR experiments were performed at two different time points. Gene expression analysis revealed that the relative expression levels of Cx43 and MYH7 were comparable in 2D and 3D hydrogel-based cultures (Figure 4.6). The hESC-CMs that were cultured in **25%_dPEG** hydrogels (6 mM) displayed a significantly higher cardiac troponin T, cTnT, expression than in 2D ($p < 0.05$) (Figure 4.6B). This

increase was not observed for hESC-CMs cultured in **sPEG** hydrogels (6 mM). This result could explain the differenence in spontaneous beating that was observed in **sPEG** and **25%_dPEG** (6 mM) hydrogels as the cTnT protein controls the interaction between actin and myosin that work together in cardiomyocyte contraction. Moreover, a significant increase in MYH6 expression was observed for cells in **sPEG** and **25%_dPEG** hydrogels (6 mM), in comparison to those maintained in 2D ($P<0.05$ and $P<0.01$, respectively) (Figure 4.6C). Also, a significant difference in expression of MYH7 was measured in 2D with a 17-fold increase in expression at day 28 in 2D, while in 3D in **25%_dPEG** hydrogels, a 1.5, 6 and 2-fold increase in 6 mM, 8 mM and 10 mM hydrogels, respectively, was obtained. The observation of an increase expression of MYH7 expression in 2D culture but a more subtle change in the 3D culture samples is most likely due to the variable cell density of the CMs within the hydrogels. Therefore, seeding a higher cell density within the gels or prolonging the culture time of hESC-CMs in the hydrogels in 3D is recommended to enhance the isoform transition from MYH6 to MYH7. Taken together, 14-day culture of hESC-CMs in a soft and dynamic hydrogels, **25%_dPEG** (6 mM), facilitated spontaneous beating and alignment, significantly increased expression of cTnT and MYH6 accompanied by an elongated morphology. Hence, these experiments set the stage for the further examination of our hydrogels to mature hESC-CMs.

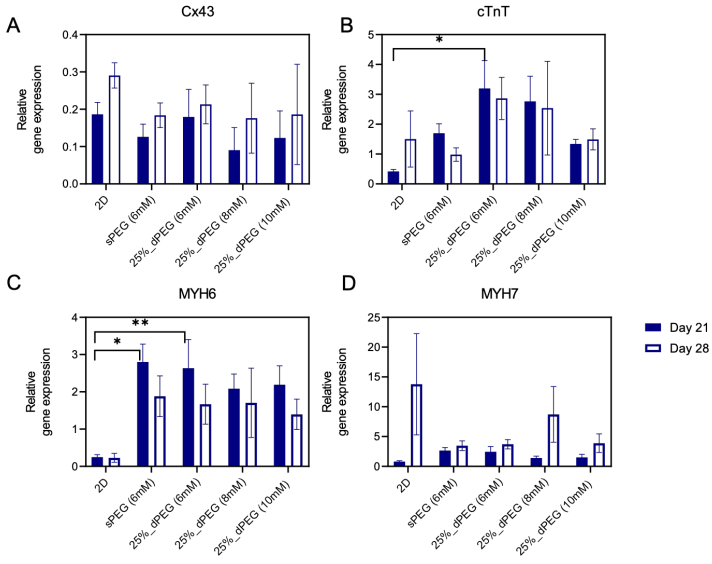

Figure 4.6. Relative gene expression profiles of hESC-CMs cultured on Matrigel in 2D for 21 and 28 days, or differentiated in 2D for 14 days and then encapsulated within 3D PEG hydrogels for another 7 days and 14 days culture. A: Cx43. B: cTnT. C: MYH6. D: MYH7. The means and standard deviations are marked inside the graphs, N = 6, *P < 0.05, ** P< 0.01.

4.4 Conclusions

A novel strategy to engineer disulfide-based hydrogel matetials using latent cyclic thiosulfinate is disclosed. Quick gelation, on the order of minutes, self-recovery and cytocompatible cell encapsulation was achieved. During 3D culture, dissolution of the hydrogel was observed when exclusively disulfide crosslinks are used. To obatin stable long-term cell culture, hydrogels with formulation of 25% dynamic crosslinks (thiol/ODT) and 75% static crosslinks (thiol/VS), or **25%_dPEG** hydrogels, needed to be employed. This ratio showed self-recovery properties, and simultaneous increase in stability over 4 weeks as shown by swelling measurements. The **25%_dPEG** hydrogels supported the culture of hESC-CMs with elongated morphologies, rapid recovery of cell spontaneous beating and cell alignment, demonstrating the crucial role of dynamic

matrix in supporting their natural behavior. Together with the significant increased expression of cardiac genes cTnT and MYH6, it is established that these materials show tremendous potential for cardiomyocytes maturation studies in the future.

4.5 References

[1] S. A. Langhans, *Front. Pharmacol.* **2018**, *9*, 1.

[2] M. Caiazzo, Y. Okawa, A. Ranga, A. Piersigilli, Y. Tabata, M. P. Lutolf, *Nat. Mater.* **2016**, *15*, 344.

[3] R. Y. Tam, L. J. Smith, M. S. Shoichet, *Acc. Chem. Res.* **2017**, *50*, 703.

[4] R. E. Michler, *Methodist Debakey Cardiovasc. J.* **2013**, *9*, 187.

[5] D. Zhang, I. Y. Shadrin, J. Lam, H. Q. Xian, H. R. Snodgrass, N. Bursac, *Biomaterials*. **2013**, *34*, 5813.

[6] S. S. Nunes, J. W. Miklas, J. Liu, R. Aschar-Sobbi, Y. Xiao, B. Zhang, J. Jiang, S. Massé, M. Gagliardi, A. Hsieh, N. Thavandiran, M. A. Laflamme, K. Nanthakumar, G. J. Gross, P. H. Backx, G. Keller, M. Radisic, *Nat. Methods.* **2013**, *10*, 781.

[7] L. Jin, T. Feng, H. Ping, R. Zerda, A. Luo, J. Hsu, A. Mahdavi, M. Sander, **2013**, *110*, 3907.

[8] S. Kim, J. Turnbull, S. Guimond, *J Endocrinol.* **2011**, *209*, 139.

[9] J. Sapudom, T. Pompe, *Biomater. Sci.* **2018**, *6*, 2009.

[10] A. Higuchi, Q. Ling, S. Hsu, A. Umezawa, *Chem. Rev.* **2012**, *112*, 4507.

[11] M. P. Lutolf, J. A. Hubbell, *Nat. Biotechnol.* **2005**, *23*, 47.

[12] C. Xu, W. Lee, G. Dai, Y. Hong, *ACS Appl. Mater. Interfaces.* **2018**, *10*, 9969.

[13] S. Ligation, E. Cambria, K. Renggli, C. C. Ahrens, C. D. Cook, C. Kroll, A. T. Krueger, B. Imperiali, L. G. Gri, *Biomacromolecules.* **2015**, *16*, 2316.

[14] G. P. Raeber, M. P. Lutolf, J. A. Hubbell, *Biophys. J.* **2005**, *89*, 1374.

[15] M. W. Tibbitt, *Mater. Today Chem.* **2019**, *12*, 16.

[16] T. E. Brown, B. J. Carberry, B. T. Worrell, O. Y. Dudaryeva, M. K. McBride, C. N. Bowman, K. S. Anseth, *Biomaterials* **2018**, *178*, 496.

[17] Z. Wei, S. Gerecht, *Biomaterials* **2018**, *185*, 86.

[18] E. Hui, K. I. Gimeno, G. Guan, S. R. Caliari, *Biomacromolecules* **2019**, *20*, 4126.

[19] S. Tang, H. Ma, H. C. Tu, H. R. Wang, P. C. Lin, K. S. Anseth, *Adv. Sci.* **2018**, *5*, 1.

[20] G. A. Barcan, X. Zhang, R. M. Waymouth, *J. Am. Chem. Soc.* **2015**, *137*, 5650.

[21] C. M. Madl, S. C. Heilshorn, *Chem. Mater.* **2019**, *31*, 8035.

[22] S. Mukherjee, M. R. Hill, B. S. Sumerlin, *Soft Matter* **2015**, *11*, 6152.

[23] M. D. Konieczynska, J. C. Villa-Camacho, C. Ghobril, M. Perez-Viloria, K. M. Tevis, W. A. Blessing, A. Nazarian, E. K. Rodriguez, M. W. Grinstaff, *Angew. Chemie* **2016**, *128*, 10138.

[24] Z. Wei, D. M. Lewis, Y. Xu, S. Gerecht, *Adv. Healthc. Mater.* **2017**, *6*, 1.

[25] P. K. Sharma, S. Taneja, Y. Singh, *ACS Appl. Mater. Interfaces* **2018**, *10*, 30936.

[26] L. L. Wang, C. B. Highley, Y. C. Yeh, J. H. Galarraga, S. Uman, J. A. Burdick, *J. Biomed. Mater. Res. - Part A* **2018**, *106*, 865.

[27] L. Cai, R. E. Dewi, S. C. Heilshorn, *Adv. Funct. Mater.* **2015**, *25*, 1344.

[28] C. Han, H. Zhang, Y. Wu, X. He, X. Chen, *Sci. Rep.* **2020**, *10*, 14997.

[29] C. B. Rodell, J. W. M. Jr, S. M. Dorsey, R. J. Wade, L. L. Wang, Y. J. Woo, J. A. Burdick, *Adv. Funct. Mater.* **2015**, *25*, 636.

[30] L. Ouyang, C. B. Highley, C. B. Rodell, W. Sun, J. A. Burdick, *ACS Biomater. Sci. Eng.* **2016**, *2*, 1743.

[31] H. Clevers, P. Matthias, *Nat. Publ. Gr.* **2016**, *539*, 560.

[32] J. A. Bums, G. M. Whitesides, *J. Am. Chem. Soc.* **1990**, *112*, 6296.

[33] R. Singh, G. M. Whitesides, *J. Am. Chem. Soc.* **1990**, *112*, 6304.

[34] D. P. Donnelly, J. N. Agar, S. A. Lopez, *Chem. Sci.* **2019**, *10*, 5568.

[35] X. Zhang, R. M. Waymouth, *J. Am. Chem. Soc.* **2017**, *139*, 3822.

[36] C. Tong, J. A. J. Wondergem, D. Heinrich, R. E. Kieltyka, *ACS Macro Lett.* **2020**, 882.

[37] D. P. Donnelly, M. G. Dowgiallo, J. P. Salisbury, K. C. Aluri, S. Iyengar, M. Chaudhari, M. Mathew, I. Miele, J. R. Auclair, S. A. Lopez, R. Manetsch, J. N. Agar, *J. Am. Chem. Soc.* **2018**, *140*, 7377.

[38] X. Marat, K. Lucet-Levannier, L. Marrot, **2013**, U.S. Patent No. US8530511B2.

[39] P. Nagy, *Antioxidants Redox Signal.* **2013**, *18*, 1623.

[40] M. D. Konieczynska, M. W. Grinstaff, *Acc. Chem. Res.* **2017**, *50*, 151.

[41] S. A. Stewart, M. B. Coulson, C. Zhou, N. A. D. Burke, H. D. H. Stöver, *Soft Matter* **2018**, *14*, 8317.

[42] K. Ronaldson-bouchard, P. Stephen, K. Yeager, T. Chen, L. Song, D. Sirabella, K. Morikawa, D. Teles, M. Yazawa, G. Vunjak-Novakovic, *Nature*. **2018**, *556*, 239.

[43] C. Xu, Y. Li, Y. Chen, C. Priest, M. A. Laflamme, W. Zhu, B. Van Biber, L. Hegerova, K. Delavan-, J. Lebkowski, J. D. Gold, *Regenerative Medicine*. **2011**, *6*, 53.

[44] L. Van Den Brink, K. O. Brandão, L. Yiangou, M. P. H. Mol, C. Grandela, C. L. Mummery, A. O. Verkerk, R. P. Davis, *Stem Cell Res.* **2020**, *43*, 101698.

[45] K. Shapira-schweitzer, D. Seliktar, *Acta Biomater*. **2007**, *3*, 33.

4.6 Supporting information

4.6.1 Materials

Tetra-arm hydroxy-terminated PEG (Mw 10 kDa) and thiol-terminated PEG (Mw 10 kDa) were obtained from Creative PEGWorks and Jenkem Technology, respectively. Poly(ethylene glycol) (Mw 6 kDa) and α,Ω-Bis-mercapto poly(ethylene glycol) (Mw 6 kDa) were purchased from Fluka and Iris Biotech GMBH. Deuterated dimethyl sulfoxide (DMSO-d_6) and chloroform ($CDCl_3$) were purchased from Eurisotop. All other chemicals and reagents for synthesis were purchased from Sigma Aldrich and used without further purification. Dulbecco's modified Eagle medium (DMEM) was from Gibco, Life Technologies. Vitronectin XF™, Essential 8™ medium and Ethylenediaminetetraacetic acid disodium salt (EDTA) were purchased from ThermoFisher Scientific. Dulbecco's Phosphate Buffered Saline (DPBS), calcein AM (AM = acetoxymethyl) and propidium iodide (PI) were obtained from Sigma-Aldrich.

4.6.2 Instruments

^1H NMR and ^{13}C NMR spectra were acquired on a Bruker DMX-400 and Bruker DPX-300 MHz at 298K. LC-MS analysis was performed on a TSQ Quantum Access MAX system equipped with a Gemini 3 µm C18 110 Å 50×4.60 mm column (UV detection at 214 nm and 254 nm, mass detection range: 160 to 3000 (Da)). The mobile phase consisted of a gradient of 10-90% of H_2O-ACN with 0.1% trifluoroacetic acid (TFA) over 13.5 minutes. HPLC purification of the monomers was executed on setup equipped with C18 column. A gradient from 10%-90% ACN (0.1% TFA) in H_2O (0.1% TFA) over 15 min at a flow rate of 12 mL/min was used. Oscillatory rheology experiments were executed on a Discovery HR-2 hybrid rheometer using a cone-plate geometry (40 mm, 1.995°) at 37 ± 0.2 °C with a peltier-based temperature controller and solvent trap. High resolution mass spectra (HR-MS) were collected on a Thermo Fisher LTQ Orbitrap mass

spectrometer equipped with an electrospray ion source in positive mode (resolution R = 60000). The spectra were collected by direct injection of samples (2 µM in H_2O-ACN 50/50 v/v) and recorded with a mass range of 150-2000 and dioctylpthalate (m/z = 391.28428) as a "lock mass". Confocal fluorescent images were acquired on Leica TCS SP8 and SPE confocal laser scanning microscopes equipped with a 10× air objective and a 40× oil immersion objective. Images were processed using the Fiji Image J software. Real-time polymerase chain reaction (RT-PCR) measurements were performed on an ABI PRISM 7700 machine (Applied Biosystems®) using SYBR Green technology.

4.6.2 Synthetic procedures

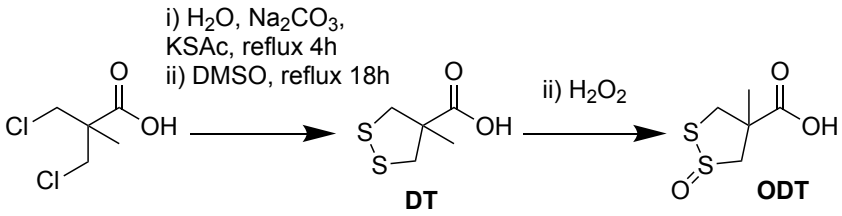

Scheme S4.1. Synthesis route of cyclic 1,2-dithiolane (**DT**) and cyclic 1,2-thiosulfinates (**ODT**)

Synthesis of DT. The synthesis of **DT** was performed as previously reported.[1] Briefly, 3,3-dichloropivalic acid (4.00 g, 23.39 mmol) was suspended in water (40 mL) within a 3-neck round bottom flask. Sodium carbonate (2.38 g, 22.46 mmol) was slowly added, followed by potassium thioacetate (5.38 g, 47.11 mmol). The resulting clear solution was heated to 100 °C, followed by the addition of sodium carbonate (7.8 g, 73.59 mmol). After refluxing overnight, DMSO (4 mL) was added and left to stir for another 12 h at 100 °C. The reaction mixture (pH ~ 9) was allowed to cool to room temperature and was acidified with hydrochloric acid (pH ~ 1). The yellow precipitate was filtered off and washed with ice-cold water and dried overnight in an vacuum oven to obtain as **DT** a yellow solid. Yield: 62.5%, 2.4 g. ^{1}H-NMR (DMSO-d_6, 400 MHz): 3.57-3.54 (d, 2H),

2.99-2.97 (d, 2H), 1.38 (s, 3H). ^{13}C-NMR (DMSO-d_6, 100 MHz): 175.42, 56.95, 46.97, 23.19.

Synthesis of ODT. Synthesis of **ODT** was performed according to a previously published protocol.[1][2] Compound **A** (3.0 g, 18.3 mmol) was dissolved in acetone (30 mL). Hydrogen peroxide aqueous solution (50%, 1.3 mL, 22.9 mmol) was added into the solution. The reaction mixture was stirred at room temperature for 24h, followed by a concentrate by N_2 flow. Afterwards, the crude was purified by flash column chromatography on silica gel with 20% EtOAc in PE. The purified fractions were collected, evaporated and dried in vacuum oven overnight to obtain **ODT** as a white solid. Yield: 47.1%, 1,55 g. ^{1}H-NMR (DMSO-d_6, 400 MHz): major isomer 4.40-4.36 (d, 1H), 3.82-3.74 (q, 2H), 3.11-3.08 (d, 1H), 1.57 (s, 3H); minor isomer 4.22-4.19 (d, 1H), 3.97-3.94 (q, 1H), 3.43-3.40 (d, 1H), 3.32-3.29 (d, 1H), 1.50 (s, 3H). ^{13}C-NMR (DMSO-d_6, 100 MHz): major isomer 174.65, 71.59, 58.66, 46.17, 23.43; minor isomer 174.32, 70.44, 56.39, 44.67, 21.59 HR-MS: $[M+H]^+$: calcd: 180.9988, found: 180.9986.

Synthesis of PEG-4DT. DT (0.20 g, 1.21 mmol) and N,N'-dicyclohexylcarbodiimide (0.25 g, 1.21 mmol) were dissolved in dry $CHCl_3$ (5 mL) and stirred at room temperature for 30 min as solution one. In a separate flask, tetra-arm hydroxyl-terminated PEG (Mw 10k) (0.30 g, 0.03 mmol) and 4-dimethylaminopyridine (15 mg, 0.12 mmol) were dissolved in dry $CHCl_3$ (5 mL). Subsequently, the PEG solution was added dropwise into the **DT** containing solution one and the reaction mixture were left stirring at room temperature for 24 h. The crude reaction mixture was first filtered prior to precipitation in cold diethyl ether, washed, re-dissolved in DCM, and re-precipitated from cold diethyl ether. The obtained products after three rounds of precipitation were re-dissolved in water, dialyzed against water for 48 h and lyophilized to obtain **PEG-4DT** as a light yellow solid. Yield: 83.3%, 0.25 g. ^{1}H-NMR ($CDCl_3$, 400 MHz): 4.29-4.27 (m, 2H), 3.80-3.44 (m, 224H), 2.93-2.90 (m, 2H), 1.47 (s, 3H).

Synthesis of PEG-4ODT. ODT (0.48 g, 2.69 mmol) and N,N'-dicyclohexylcarbodiimide (0.632 g, 3.06 mmol) were dissolved in dry DMF (10 mL) and stirred at room temperature for 30 min. In a separate flask, tetra-arm hydroxyl-terminated PEG (Mw 10k) (1.15 g, 0.11 mmol) and 4-dimethylaminopyridine (60 mg, 0.50 mmol) were dissolved in dry DMF/DCM (10 mL, 1:1, v/v). Subsequently, the PEG solution was added dropwise into the **ODT** solution and the reaction mixture was left stirring at room temperature for 24 h. The reaction crude was first filtered and the filtrate was precipitated in cold diethyl ether, washed, re-dissolved in DCM, and precipitated from cold diethyl ether. The obtained products after three rounds precipitation were re-dissolved in water, dialyzed against water for 48 h and lyophilized to obtain **PEG-4ODT** as a white solid. Yield: 82.6%, 0.95 g. ^{1}H-NMR ($CDCl_3$, 400 MHz): 4.53-4.49 (m, 1H), 4.29-4.27 (m, 2H), 3.90 (d, 1H), 3.81-3.44 (m, 224H), 3.04-3.00 (d, 1H), 2.95-2.87 (d, 1H), 1.68 (s, 3H).

Synthesis of PEGdiODT. ODT (0.32 g, 1.76 mmol) and N,N'-dicyclohexylcarbodiimide (0.40 g, 1.94 mmol) were dissolved in dry DMF (10 mL) and stirred at room temperature for 30 min. In a separate flask, linear hydroxyl-terminated PEG (Mw 6k) (1.18 g, 0.20 mmol) and 4-dimethylaminopyridine (121 mg, 0.99 mmol) were dissolved in dry DMF/DCM (10 mL, 1:1, v/v). Subsequently, the PEG solution was added dropwise into the **ODT** solution and the reaction mixture was left stirring at room temperature for 24 h. The reaction crude was first filtered and the filtrate was precipitated from cold diethyl ether, washed, dissolved in DCM, and re-precipitated from cold diethyl ether. The obtained products after three rounds precipitation were re-dissolved in water, dialyzed against water for 48 h and lyophilized to obtain **PEGdiODT** as a white solid. Yield: 75.4%, 0.89 g. ^{1}H-NMR ($CDCl_3$, 400 MHz): 4.53-4.49 (m, 2H), 4.32-4.27 (m, 4H), 3.93-3.90 (d, 2H), 3.82-3.44 (m, 540H), 3.04-3.01 (m, 2H), 1.69 (s, 3H).

Peptide synthesis. RGD peptides (CGGGRGDS) (cRGD) were synthesized on an automatic CEM peptide synthesizer on a 100 µmol scale. Fmoc-Rink amide AM resin

with a loading of 0.74 mmol/g was used. Fmoc-Rink amide AM resin with a loading capacity of 0.74 mmol/g was used. Amino acid coupling was performed with 4 eq. of the amino acid, 4 eq. of the activator HCTU and 8 eq. of DIPEA. Fmoc-deprotection was executed using a solution of pyridine and dimethylformamide (DMF) (2:8 v/v). The peptides were cleaved from the resin using a TFA solution containing 2.5% H_2O, 2.5% 1,2-ethanedithiol and 2.5% triisopropylsilane (TIPS) for 3h, precipitated in cold diethyl ether, dried, dissolved in water and purified by HPLC using a gradient 1-10% ACN/H_2O over 15 min. The product was concentrated by evaporation and lyophilized overnight to obtain a white solid. LC-MS: t =0.65 min, m/z calcd: 604.26, found: 603.07.

4.6.3 Hydrogel preparation

Hydrogels were prepared by separately dissolving PEG macromers in PBS (pH 7.4) and mixing them in the desired molar ratio. Specifically, to prepare the thiol/ODT crosslinked hydrogel, stock solution of **PEG-4ODT** (100 µL) was mixed with a freshly prepared solution of **PEG-4SH** (100 µL), and pipetted to obtain a homogeneous solution with a final PEG macromer concentrations in the range of 1-12 mM. The precursor solution was left at room temperature to gelate. Hydrogels with static crosslinks (**PEG-4VS** and **PEG-4SH**) and with linear PEG macromers (**PEGdiODT** and **PEGdiSH**) were prepared in the same way. To prepare the hybrid hydrogels, stock solutions of **PEG-4ODT** (60 µL) and **PEG-4VS** (60 µL) were mixed with freshly prepared solutions of **PEG-4SH** (60 µL), and pipetted to obtain a homogeneous solution with final PEG macromer concentrations between 4.5-10 mM. The precursor solution was left at room temperature for gelation. Gelation time was determined until the gel did not flow on vial inversion.

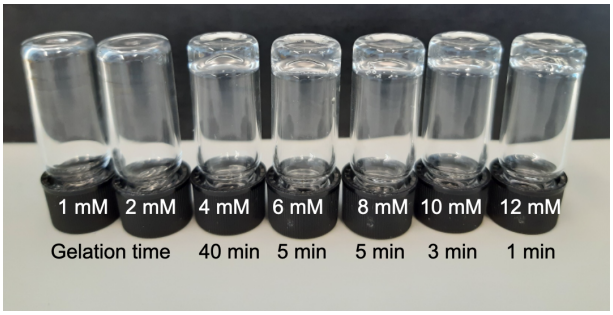

Figure S4.1. Gel inversion test of **ODT-SH** hydrogels prepared from macromers **PEG-4ODT** and **PEG-4SH** with thiol/ODT molar ratio at 1:1.

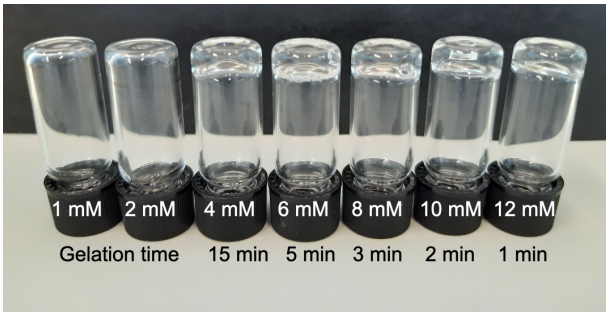

Figure S4.2. Gel inversion test of **ODT-SH** hydrogels prepared from macromers **PEG-4ODT** and **PEG-4SH** with thiol/ODT molar ratio at 2:1.

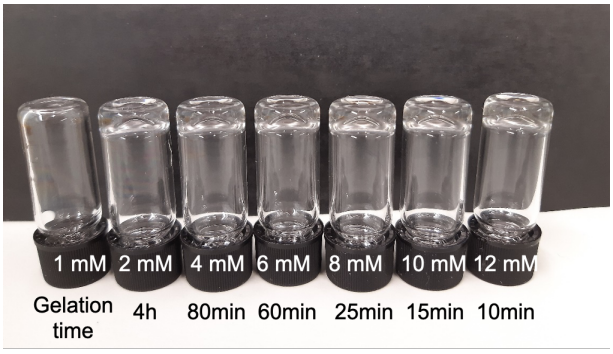

Figure S4.3. Gel inversion test of **VS-SH** hydrogels prepared from macromers **PEG-4VS** and **PEG-4SH** with thiol/VS molar ratio at 1:1.

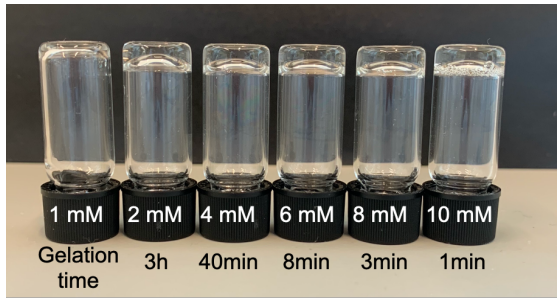

Figure S4.4. Gel inversion test of **25%_dPEG** hydrogels prepared from macromers **PEG-4ODT**, **PEG-4VS** and **PEG-4SH** with thiol/ODT molar ratio at 1:1 and thiol/VS molar ratio at 1:3.

4.6.4 NMR analysis

ODT was weighed in a 2.0 mL glass vial and dissolved in deuterated water with a final concentration at 20 mM. In a separate vial, glutathione (GSH) was freshly weighed and dissolved in deuterated water with final concentrations at 20 mM, 40 mM, 60 mM and 80 mM, respectively. The **ODT** solution (300 µL) was mixed with freshly prepared GSH solution (300 µL) by vortex for 10 s prior to its transfer into a NMR tube. The samples were incubated at 37 ˚C until desired time points and NMR spectra were collected on a Bruker DMX-400 at 298K.

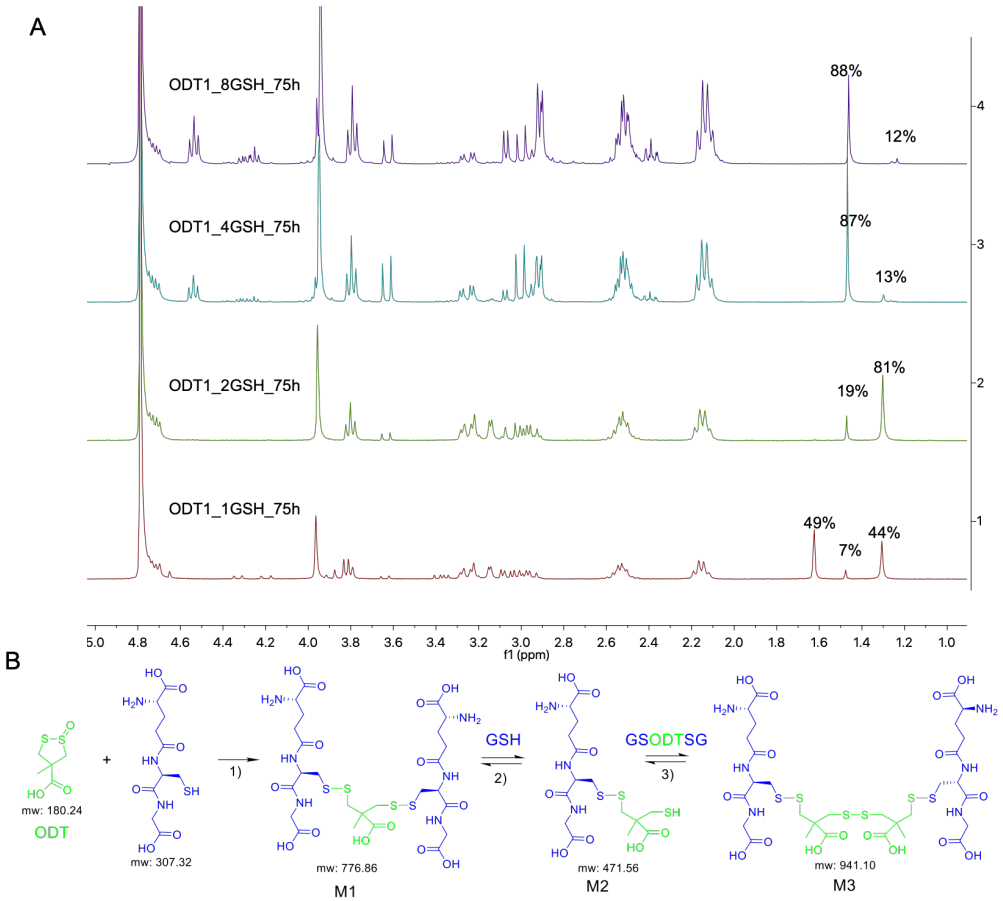

Figure S4.5. A) ^{1}H-NMR spectra of **ODT** and GSH mixture after 75-h incubation at 37˚C. B) Proposed mechanism of thiol (blue) and cyclic thiosulfinates (green) crosslinking. 1) **ODT** was reacted with GSH with in a molar ratio of 1:2 in the same mechanism reported from Agar and co-workers; [2] 2) thiol/disulfide exchange between GSH and **M1** to result in a new free thiol, **M2**; 3) further thiol/disulfide exchange to give a new disulfide product **M3**.

4.6.5 Oscillatory Rheology

Oscillatory rheology experiments were carried out on a Discovery HR-2 hybrid rheometer using parallel plate geometry (20 mm diameter) at 37 ± 0.2 °C with a peltier-based temperature controller and a solvent trap. The prepared hydrogel (100 µL) was

pipetted onto the bottom plate and the geometry was lowered to a gap distance of 300 µm. Time sweep measurements were executed at a frequency of 1.0 Hz and strain of 0.05% and frequency sweeps were conducted from 0.01−10 Hz with 0.05% strain. Subsequently, a step-strain measurement was performed after a plateau was reached in the storage modulus during the time sweep. Then, 700% strain was applied on the hydrogels for 300 s. The hydrogels were left to recover for 300 s while measuring at 0.05% strain (f = 1.0 Hz) and continued with a frequency sweep (from 0.01 to 10 Hz, γ = 0.05%), during which the storage modulus returned to the original plateau. This measurement was repeated for three cycles.

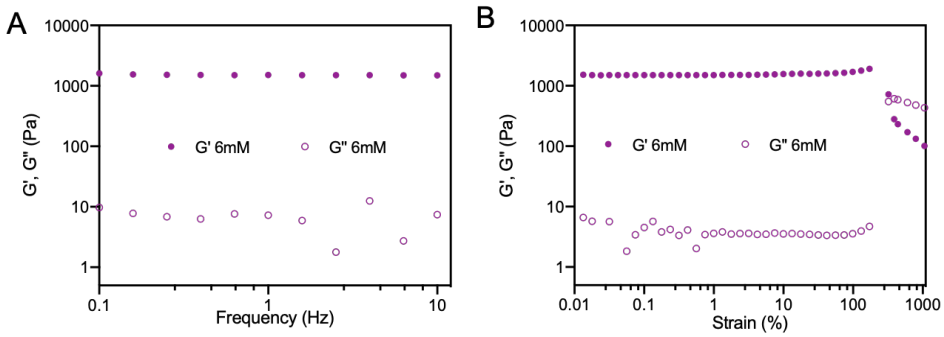

Figure S4.6. A) Frequency sweep measurements of **ODT-SH** hydrogels in PBS (pH 7.4) at 25 ± 0.2 °C. Frequency sweep data was collected in a range of 0.01 Hz to 10 Hz with strain of 0.05%. B) Amplitude sweep measurements of **ODT-SH** hydrogels (6 mM) in PBS (pH 7.4) at 25 ± 0.2 °C with frequency of 1 Hz and strain from 0.1% to 1000%.

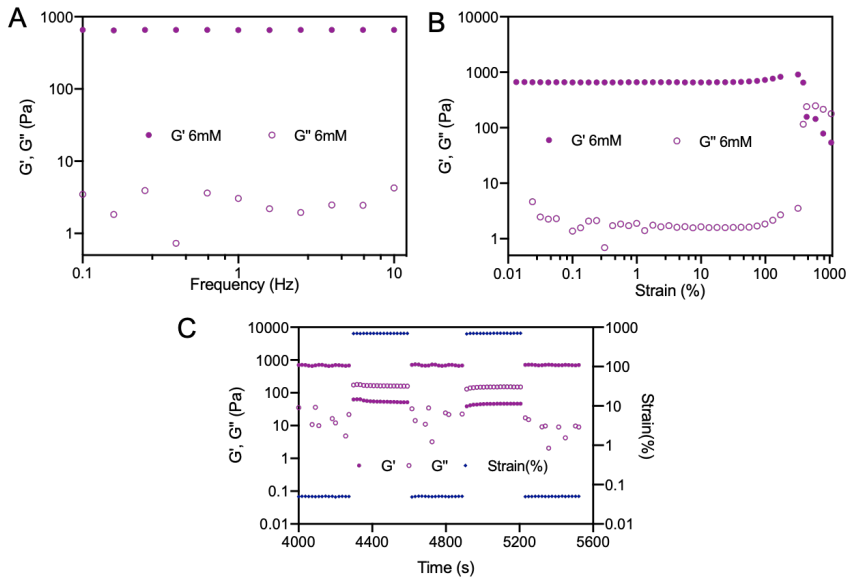

Figure S4.7. A) Frequency sweep measurement of **ODT-SH** hydrogels (6 mM) in PBS (pH 7.4) at 37 ± 0.2 °C. Frequency sweep data was collected in a range of 0.01 Hz to 10 Hz with strain of 0.05%. B) Amplitude sweep measurements of **ODT-SH** hydrogels (6 mM) in PBS (pH 7.4) at 37 ± 0.2 °C with frequency of 1 Hz and strain from 0.1% to 1000%. C) Step-strain measurements of **ODT-SH** hydrogels (6 mM) at 37 ± 0.2˚C with a frequency of 1 Hz; Low (0.05%) and high strain (700%) were applied alternatively for two cycles.

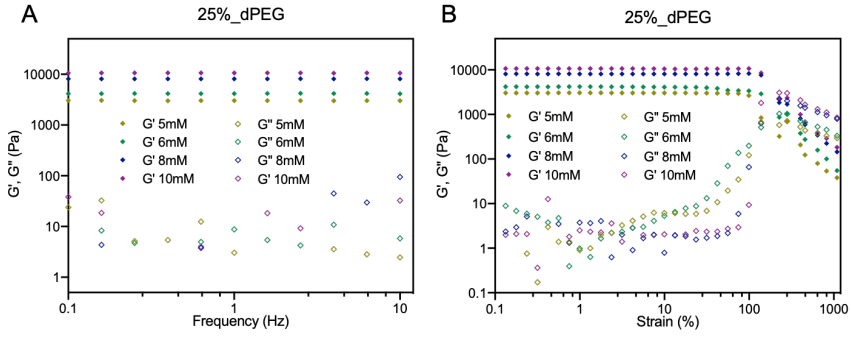

Figure S4.8. A) Frequency sweep measurements of **25%_dPEG** hydrogels in PBS (pH 7.4) at 37 ± 0.2 °C. Frequency sweep data were collected in a range of 0.1 Hz to 10 Hz with strain of 0.05%. B) Amplitude sweep measurements of **25%_dPEG** hydrogels at 37 ± 0.2 °C with frequency of 1 Hz and strain from 0.1% to 1000%.

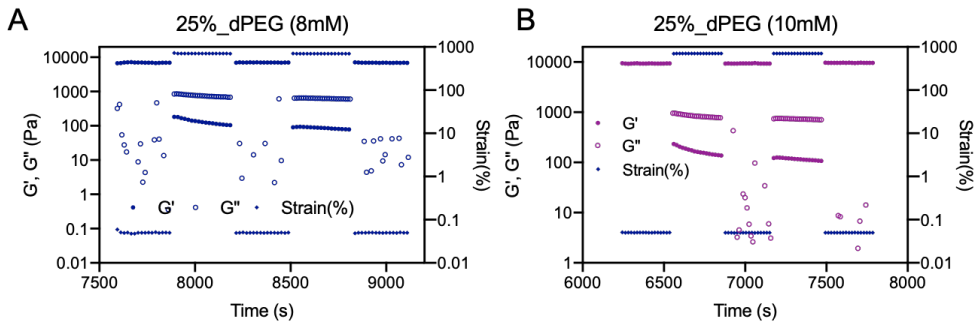

Figure S4.9. Step-strain measurement of **25%_dPEG** hydrogels in PBS (pH 7.4) at 37 ± 0.2 °C. Low strain (0.05%) and high strain (700%) were alternated twice in a sequence for 300 s applied twice for 120s. The data was collected at a frequency of 1 Hz.

4.5.6 Swelling measurements

Hydrogels (200 µL) were prepared according to gelation protocol descripted above and were allowed to stand for 2h. The wet weight of hydrogels were measured as W_0. Afterwards, DMEM medium (200 µL) was added on top of hydrogel and incubated at 37˚C. At desired time points, the supernatant solution was carefully removed and the wet weight of the hydrogels were measured as Wt. The percentage of hydrogel degradation or swelling ratios was calculated by the following equation: weight change (%) = W_t/W_0 x 100%.

4.5.7 LIVE/DEAD staining

NIH 3T3 cells were cultured in high glucose DMEM supplemented with 10% Fetal Calf Serum, 1% Glutamax, and 0.2% penicillin-streptomycin in a 37 °C incubator with 5% CO2. Prior to encapsulation, cells were dissociated by trypsin, collected by centrifuge and re-suspended in PBS with a final cell centration at 2 x 10^7 cells/mL. To prepare the **ODT-SH** hydrogel, **PEG-4ODT** stock solution (80 µL) was first mixed with freshly prepared cRGD (PBS, 10 µL) by pipetting. After 5 min incubation, a cell suspension (20 µL) was added and mixed, followed by the addition of a freshly prepared **PEG-4SH**

solution (90 μL). The precursor solution was mixed and pipetted into μ-Slide angiogenesis slide by 12μL/well. After incubated at 37˚C for 15 min, fresh culture medium (48 μL) was added on top and cells were cultured at 37 °C. At pre-determined time points, the medium on top of the hydrogel was removed by pipetting, rinsed twice with PBS (pH 7.4, 45 μL) and incubated with a prepared staining solution (45 μL) (calcein AM (2 μM) and propidium iodide (1.5 μM)) at 37 °C for 20 min. The staining solution was removed and the hydrogel was rinsed again with PBS two times (45μL). The stained cell-laden hydrogel was imaged through z-stack on Leica TCS SP8 confocal laser scanning microscope equipped with a 10× air objective. Fluorescent images were acquired at a resolution of 1024 × 1024 pixels using an excitation wavelength of 488 nm and an emission filter of 500−545 nm for calcein AM and an excitation wavelength of 532 nm and an emission filter of 594−686 nm for propidium iodide. Cell viability was determined by counting the calcein AM-stained green cells (viable) and PI-stained red cells (dead) in ImageJ. For each hydrogel sample at each time point, three Z-stack images were counted (~2000 cells). To prepare **25%_dPEG** hydrogel, **PEG-4ODT** stock solution (50 μL) was first mixed with freshly prepared cRGD (PBS, 10 μL) by pipetting. After 5 min incubation, **PEG-4VS** solution (50 μL) and cell suspension (20 μL) was added and mixed, following with addition of freshly prepared **PEG-4SH** solution (70 μL). The precursor solution was mixed and pipetted into μ-Slide angiogenesis slide by 12μL/well. After incubated at 37˚C for 15 min, fresh culture medium (48 μL) was added on top and cells were cultured at 37 °C. Cytocompatibility test of **25%_dPEG** hydrogels was performed in the same protocol described above.

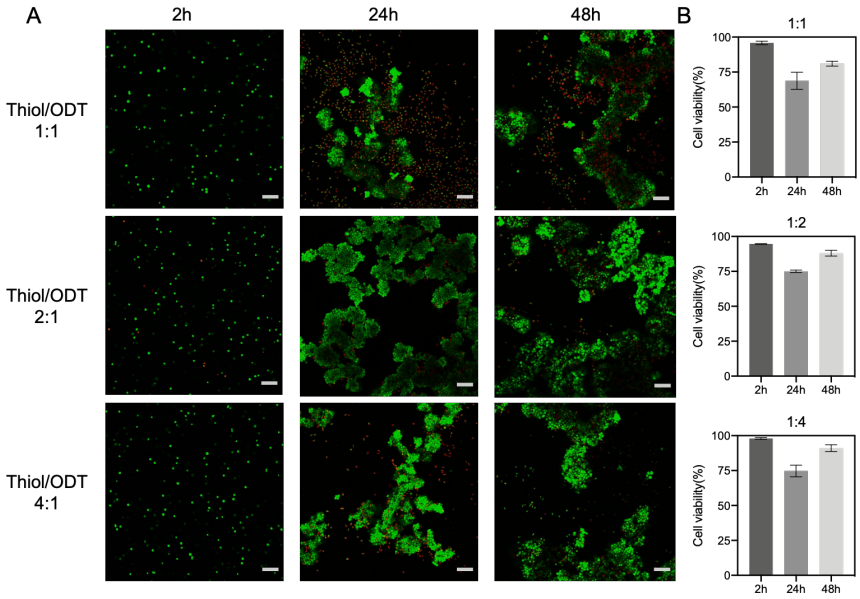

Figure S4.10. Cytocompatibility of **ODT-SH** hydrogels (6 mM) with thiol/ODT molar ratios at 1:1, 2:1 and 4:1. A) Representative z-stack images of cells in hydrogels after 2h, 24h and 48h culture. Cells were stained with calcein AM (viable cells, *green*) and propidium iodide (PI) (dead cells, *red*). Scale bar: 100 µm. B) Quantification of cell viability. Error bars represent standard deviations of means.

4.6.8 hESC culture and differentiation

Human embryonic stem cell line (hESCs) was obtained from Prof. Dr. Robert Passier in University of Twente (The Netherlands). hESCs were cultured on six-well plates coated with vitronectin. Cells were passaged by use of EDTA solution (0.5 mM) with replating densities at 180K cells/well and 100K cells/well on Mondays and Thursdays, respectively. In detail, on the passage day, cells were first washed with PBS and incubated with EDTA solution for 5 min at 37°C. After aspirating the EDTA solution, Essential 8^{TM} medium (RevitaCell 1:200, 2 mL) was added. A P1000 micropipette was used to suspend and dissociate cells (6-8 times). Cells were first collected by a 5-min centrifuge at 300g and then replated into new plates. The replated cells were treated

with medium supplied with Revita Cell (1:200) for 24h and refreshed with E8 medium and cultured until next passage.

Prior to the start of cardiomyocyte differentiation, Matrigel coated plates were prepared according to a reported protocol.[3] On the passage day, hESCs were seeded on the Matrigel coated plates and differentiated to cardiomyocytes using the STEMdiff™ Cardiomyocyte Differentiation Kit (Stem Cell Technologies). Fluorescent images of hESC-derived cardiomyocytes (hESC-CMs) were acquired on a Leica SP8 confocal microscope at predetermined time points using an excitation wavelength of 488 nm and an emission filter of 500-545 nm for GFP and an excitation wavelength of 532 nm and an emission filter of 600-680 nm for mRuby.

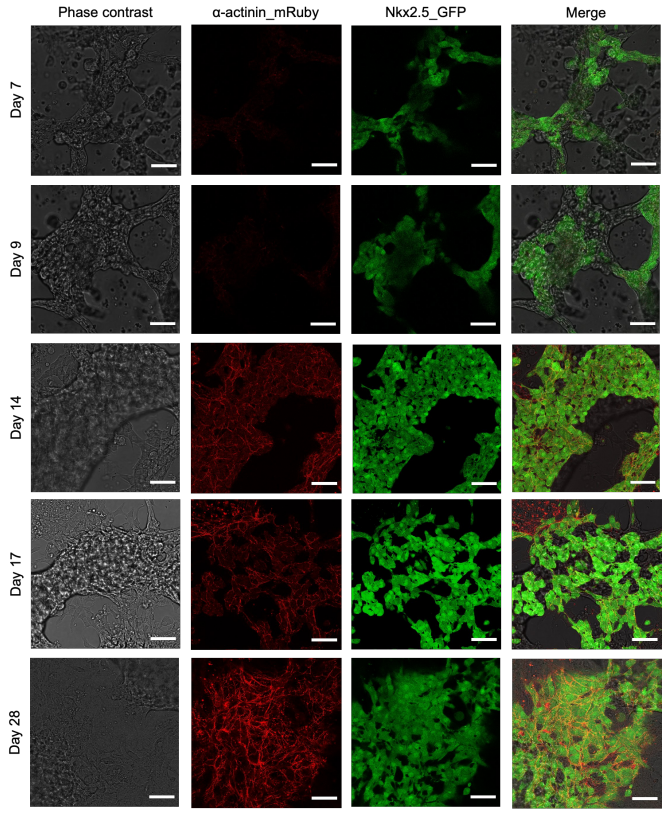

Figure S4.11. Representative images of hESC-CM differentiation on Matrigel in 2D over 28 days . Fluorescent images of cardiac transcription factor Nkx2.5_GFP (green) and the sarcomeric protein, α-actinin_mRuby (red). Brightfield microscopy images were

captured after 7, 9, 14, 17 and 28 days differentiation, respectively. Merged images were prepared in Fiji. Scale bar: 50 µm.

4.6.9 hESC-CMs encapsulation and culture in 3D

After 14-days differentiation, hESC-CMs were first washed with DPBS and then dissociated by incubation with a TrypLE Select (1x) solution for 5 min at 37 °C. The TrypLE Select solution was removed and cells were suspended in Cardiomyocyte Maintenance medium by a P1000 micropipette. (8-10 times) Then, hESC-CMs were collected, spun down and resuspended in Cardiomyocyte Maintenance medium with a cell density at 5 x 10^7 cells/mL. Afterwards, hESC-CMs were encapsulated within **25%_dPEG** hydrogels and **sPEG** hydrogel in the same way as NIH 3T3 cells. Complete cardiomyocyte maintenance medium (48 µL) was added on top of the gel and was refreshed every other day. At desired timepoints, bright field images were acquired on SP8 confocal microscope using 10x and 20x objectives. Fluorescent images were acquired at a resolution of 1024 x 1024 pixels and a z-step size of 2.00 µm, using an excitation wavelength of 488 nm and an emission filter of 500-545 nm for GFP and an excitation wavelength of 532 nm and an emission filter of 600-680 nm for mRuby.

4.6.10 RT-PCR

At pre-determined time points, cells were lysed with GTC lysis buffer (500 µL) at room temperature for 1 min and stored at -20 °C until RNA isolation was initiated. For cells released from the hydrogels, GTC (500 µL) was added and incubated at room temperature for 6 min. After that, the gels were spun down (5 min, 500g) and the supernatant was collected in a new Eppendorf tube.

Total RNA was collected using the standard phenol/chloroform extraction method and 500 ng RNA was reverse transcribed using RevertAid Reverse Transcriptase. For RT-PCR, cDNA (4 µL) was mixed with primers mix (Table S4.1) and

SensiMix SYBR low-ROX mix and analysis was performed on a 7500 Fast Real-time PCR system (Applied Biosystems). Gene expression was normalized to the averaged gene expression of two housekeeping genes, the tyrosine 3-monooxygenase/tryptophan 5-monooxygenase activation protein zeta coding gene YWHAZ and the 60S ribosomal protein L37 coding gene RPL37. Outlier tests were performed on dCt values and relative expression values (ROUT method, Q=1%). One-way ANOVA tests were used to determine significant changes in gene expression (95% confidence interval), followed by a Tukey test to determine significant changes between groups.

Table S4.1. Primer sequences used for RT-PCR

Gene	Forward 5'- 3'	Reverse 5' -3'
Sox2	TGGTTACCTCTTCCTCCCACTCCAG	TAGTGCTGGGACATGTGAAGTCTGC
Nanog	TCCAGCAGATGCAAGAACTCTCCAAC	CACCATTGCTATTCTTCGGCCAGTTG
Oct4	GCTTGGAGACCTCTCAGCCTGAG	TTTIGCTCCAGCTTCTCCTTCTCCAG
cTnT	AGTTCGACCTGCAGGAGAAGTTCAAG	TATTTCCAGCGCCCGGTGACTTTAG
Cx43	GTCTGAGTGCCTGAACTTGCCTTTTC	TCCAGCAGTTGAGTAGGCTTGAACC
MYH6	TTCGAGC CAAGAGC CGTGACATTG	TTACAGGTTGGCAAGAGTGAGGTTCC
MYH7	GTCAACAAGCTGCGGGCCAAG	CTGAGCAGATCAAGATGTGGCAAAGC
YWHAZ	TGAAGAGTCATACAAAGACAGCACGCT	TTGGAAGGCCGGTTAATTTTCCCCT
RPL37	TGGAGTGCCAAGGCTAAAAGACGAA	GGGTTTAGGTGTTGTTCCTTCACGGA

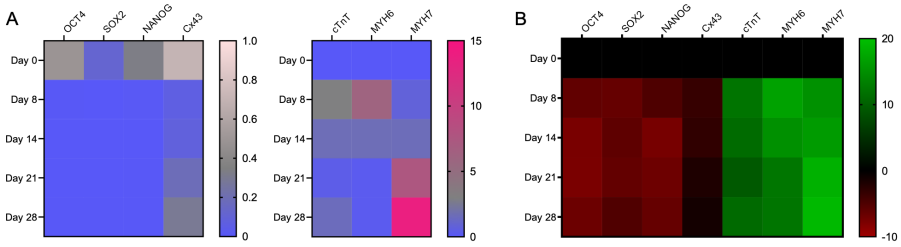

Figure S4.12 Gene expression profiles of hESC-CMs differentiation on Matrigel in 2D over 28-days. A) Relative gene expression of the pluripotency genes OCT4, SOX2 and NANOG (scale: 0-1.0) and the cardiac gene Cx43 (scale: 0-1.0), cTnT, MYH6 and MYH7 (scale: 0-15). B) C: Fold change (log2) for all genes in comparison to expression on day 0. N = 6

4.6.11 Appendix: NMR spectra

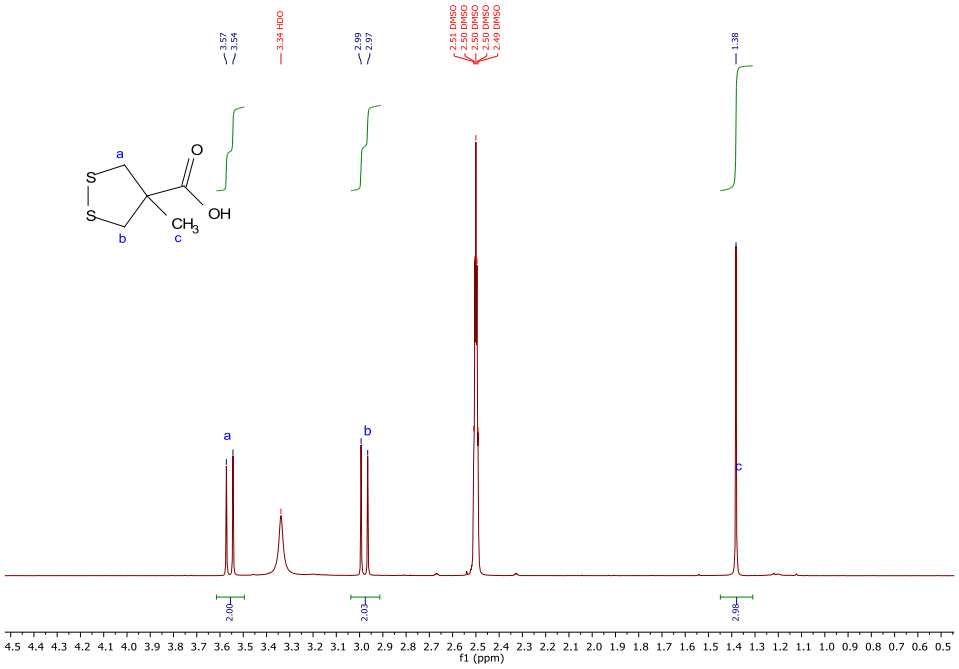

Figure A4.1. ^{1}H-NMR (400 MHz, 298K, DMSO-d_6) spectrum of **DT**

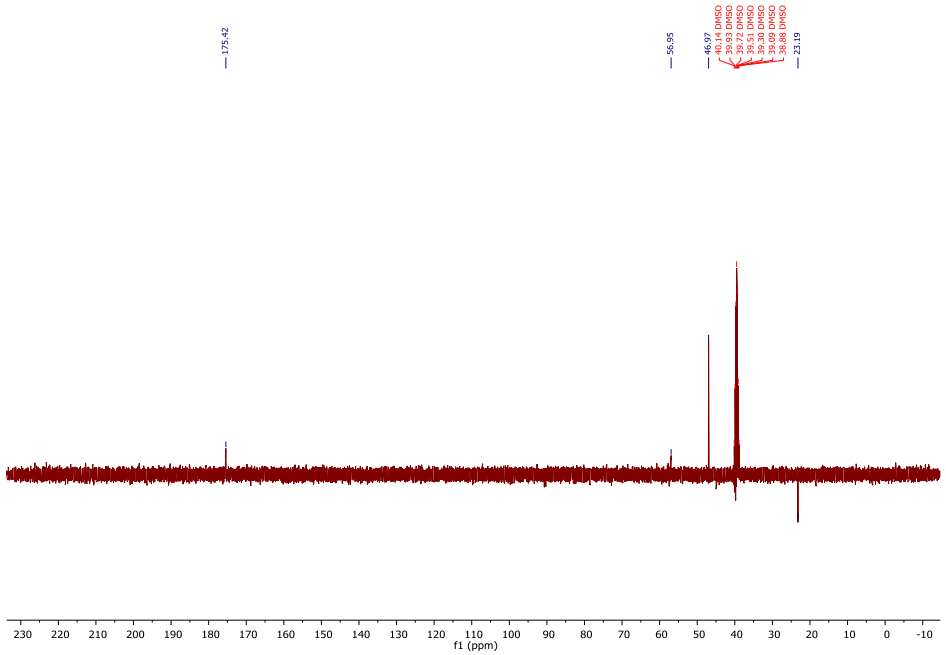

Figure A4.2. ^{13}C-NMR (400 MHz, 298K, DMSO-d$_6$) spectrum of **DT**

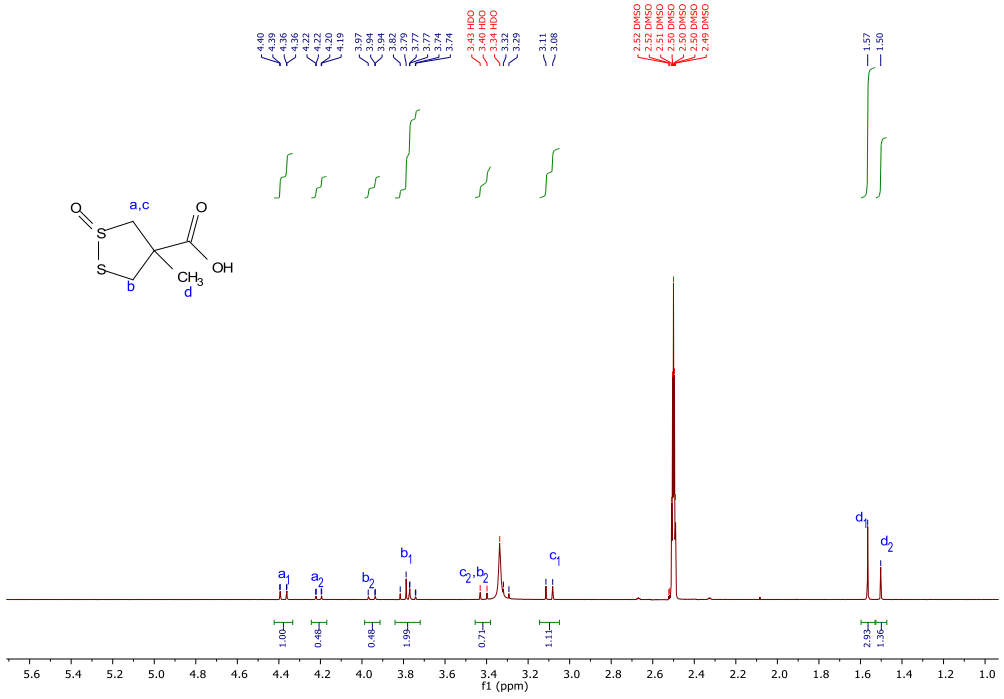

Figure A4.3. ^{1}H-NMR (400 MHz, 298K, DMSO-d$_6$) spectrum of **ODT**

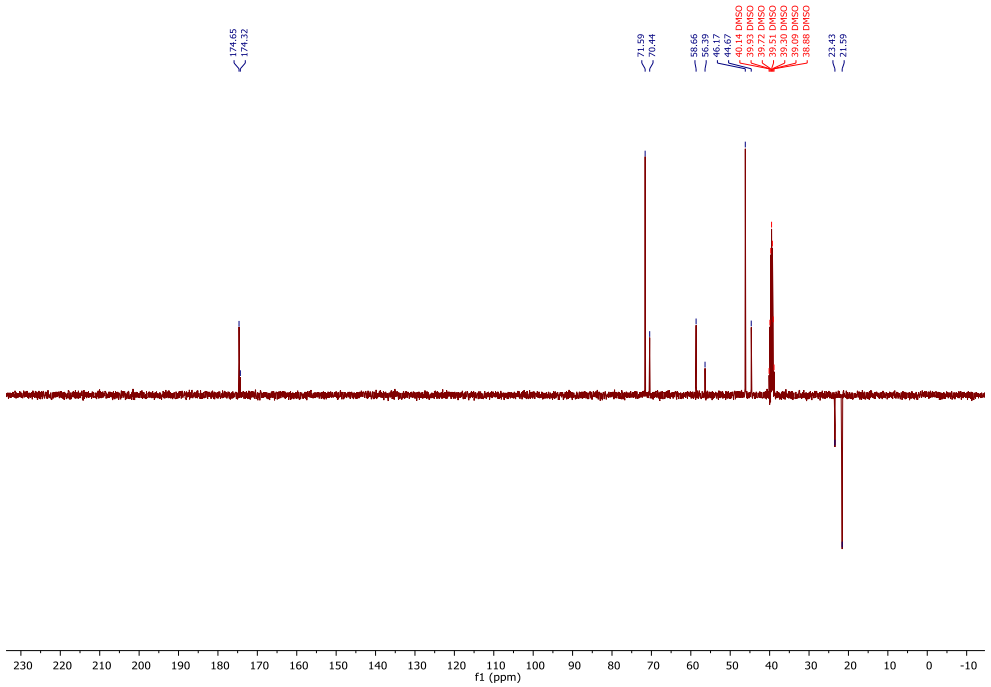

Figure A4.4. ^{13}C-NMR (400 MHz, 298K, DMSO-d_6) spectrum of **ODT**

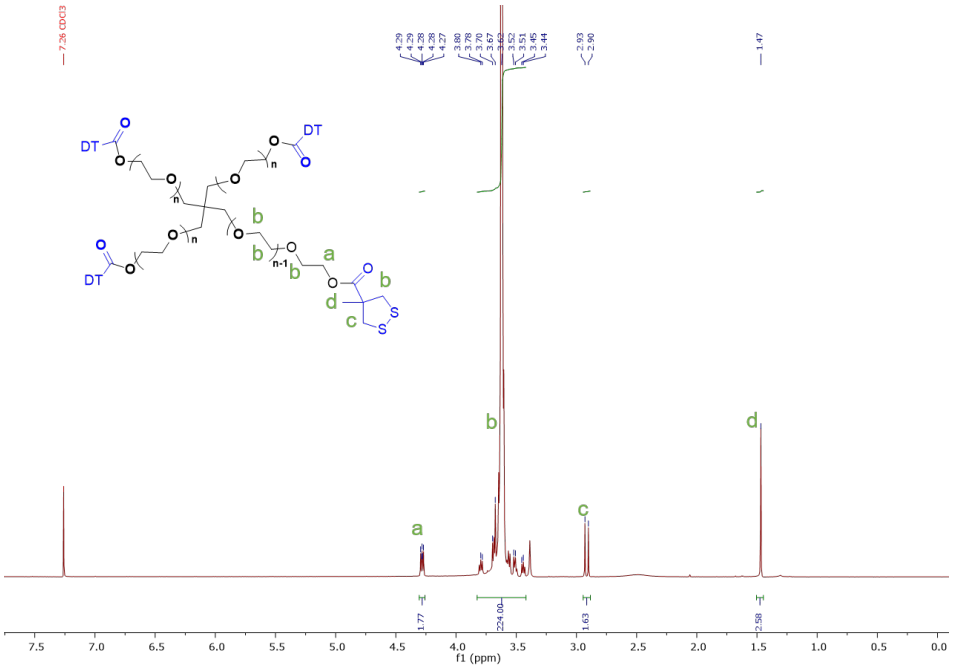

Figure A4.5. ^{1}H-NMR (400 MHz, 298K, $CDCl_3$) spectrum of **PEG-4DT**. The degree of functionalization was 86%.

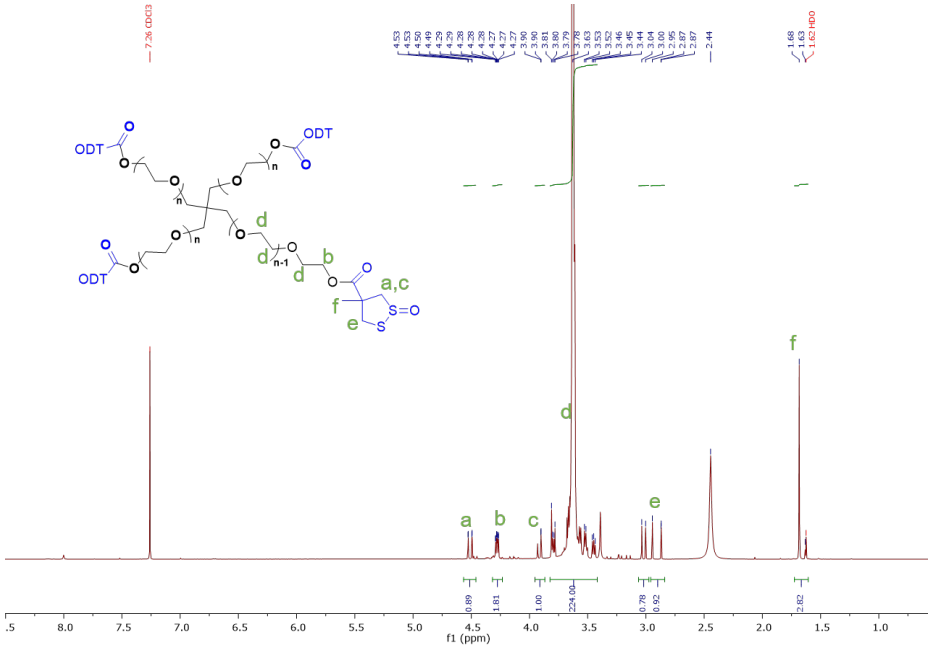

Figure A4.6. ^{1}H-NMR (400 MHz, 298K, $CDCl_3$) spectrum of **PEG4-ODT**. The degree of functionalization was 90%.

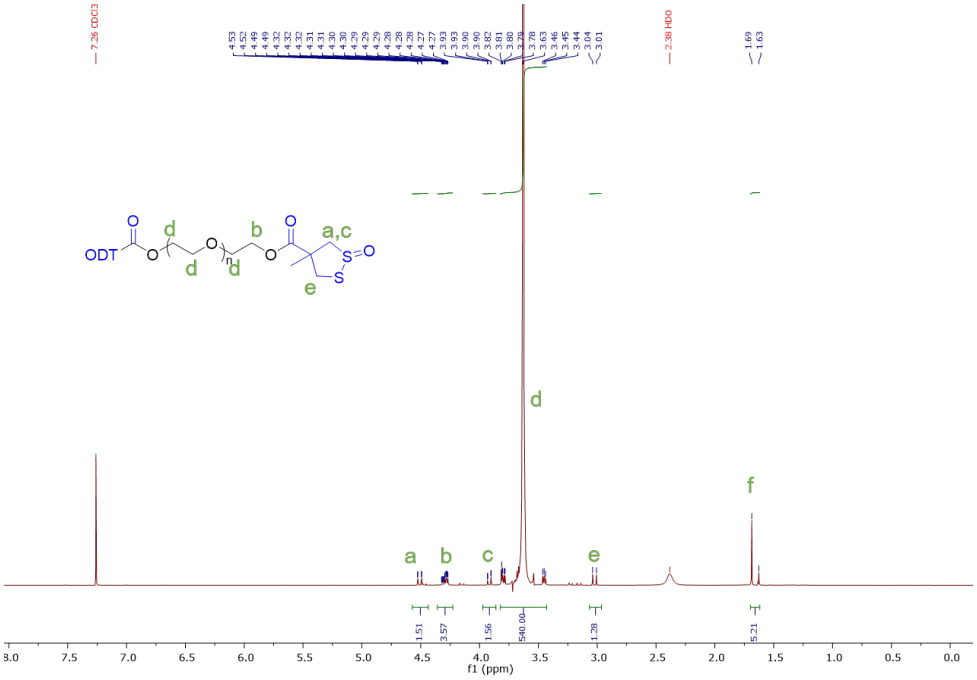

Figure A4.7. ^{1}H-NMR (400 MHz, 298K, $CDCl_3$) spectrum of **PEGdiODT**. The degree of functionalization was 86%.

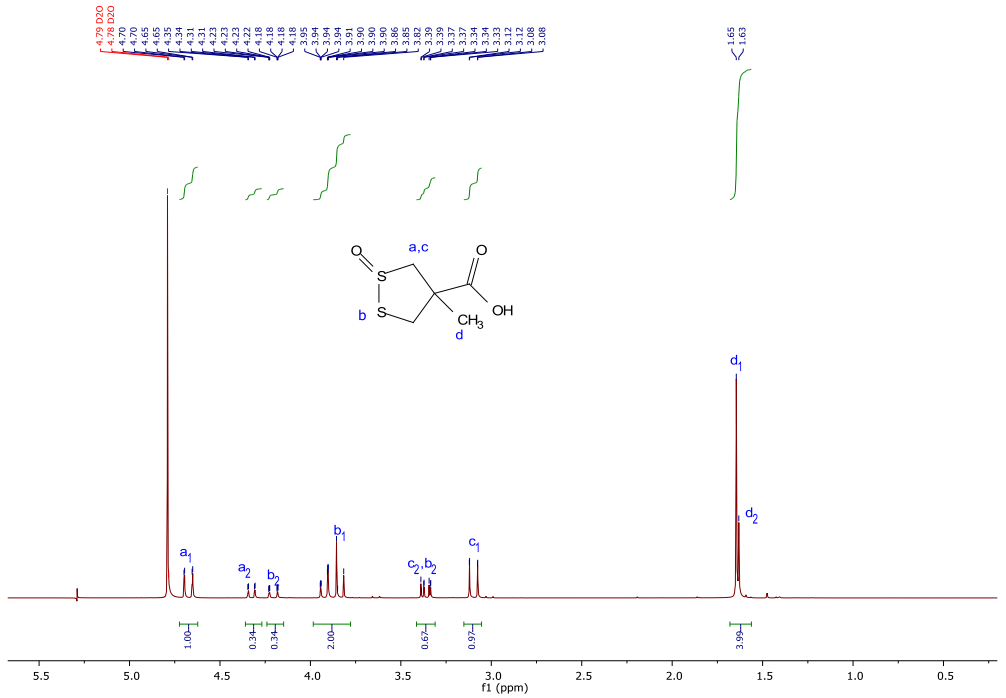

Figure A4.8. ^{1}H-NMR (400 MHz, 298K, D_2O) spectrum of **ODT**.

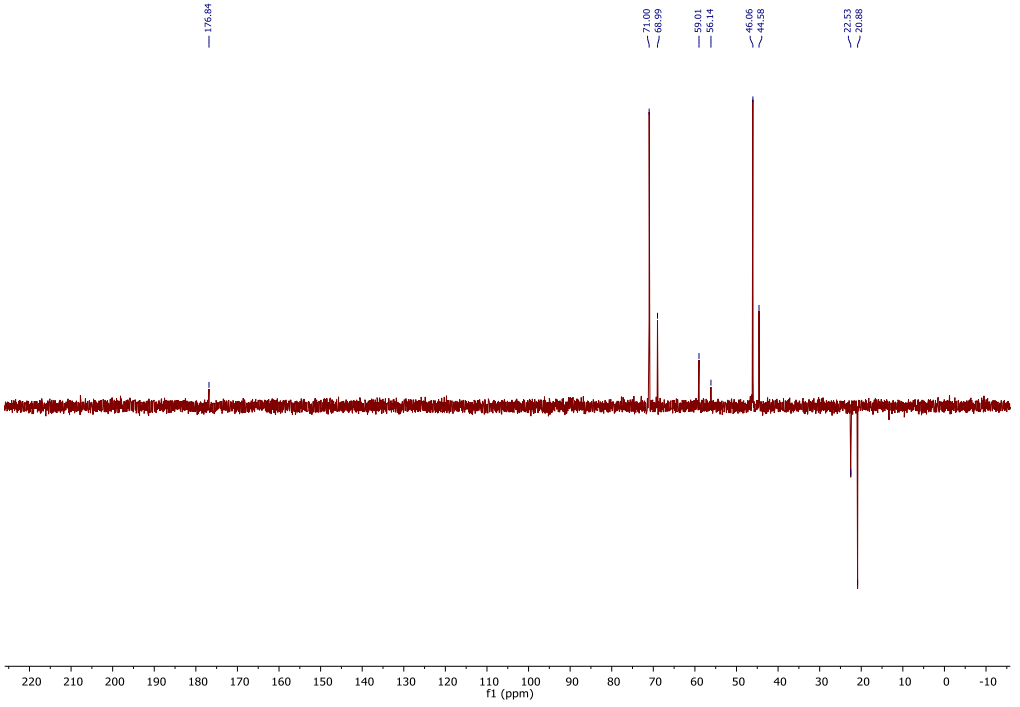

Figure A4.9. ^{13}C-NMR (100 MHz, 298K, D_2O) spectrum of **ODT**

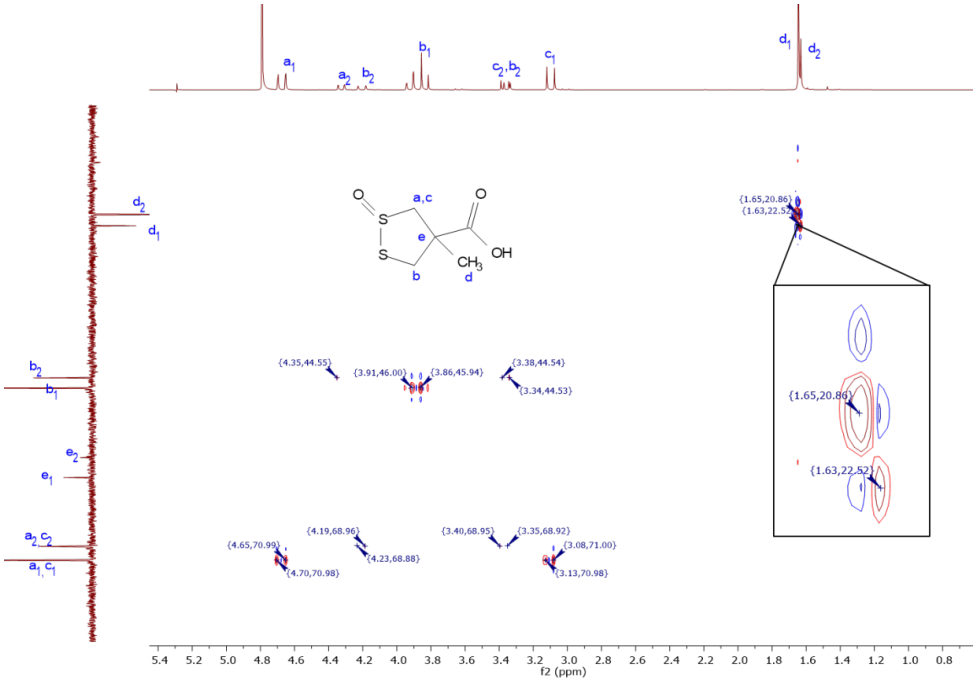

Figure A4.10. HSQC (400 MHz, 298K, D_2O) spectrum of **ODT**

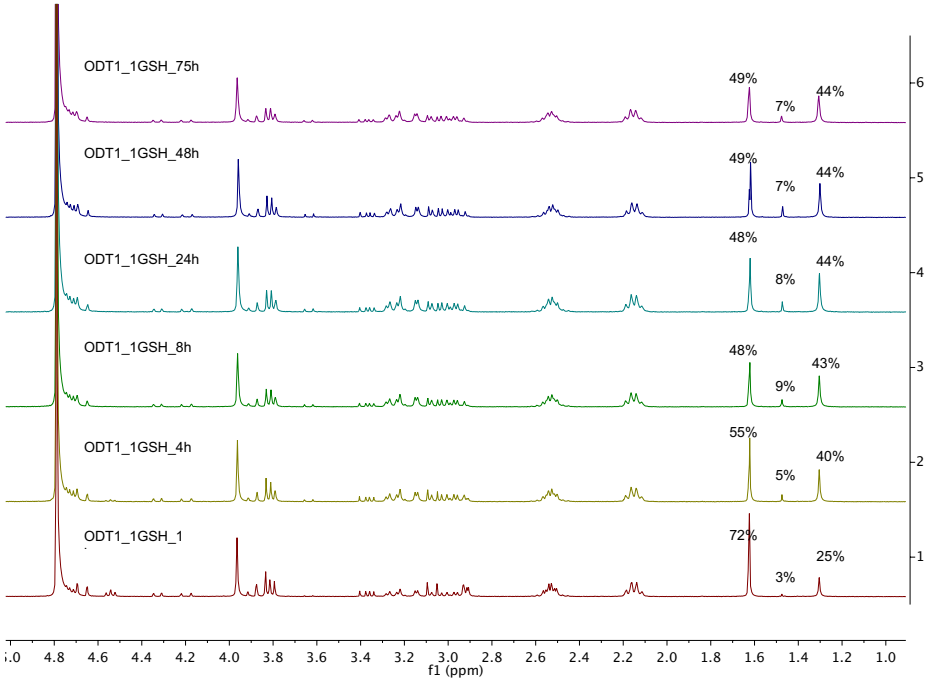

Figure A4.11. ^{1}H-NMR (400 MHz, 298K, D_2O) spectrum of the **ODT** and **GSH** mixture at specific time points with a molar ratio of thiol/ODT at 1:1

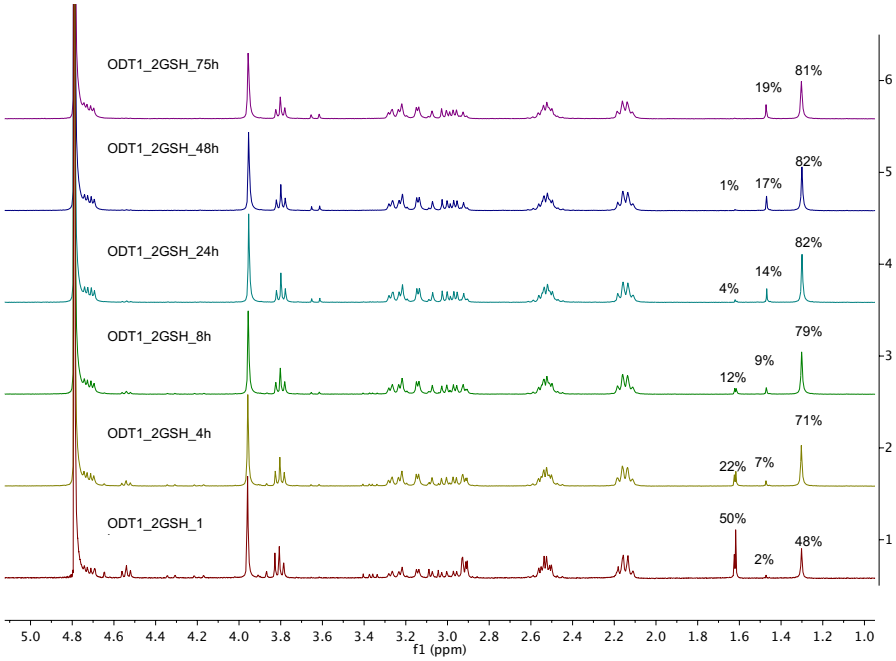

Figure A4.12. ^{1}H-NMR (400 MHz, 298K, D_2O) spectrum of the **ODT** and **GSH** mixture at specific time points with a molar ratio of thiol/ODT at 2:1

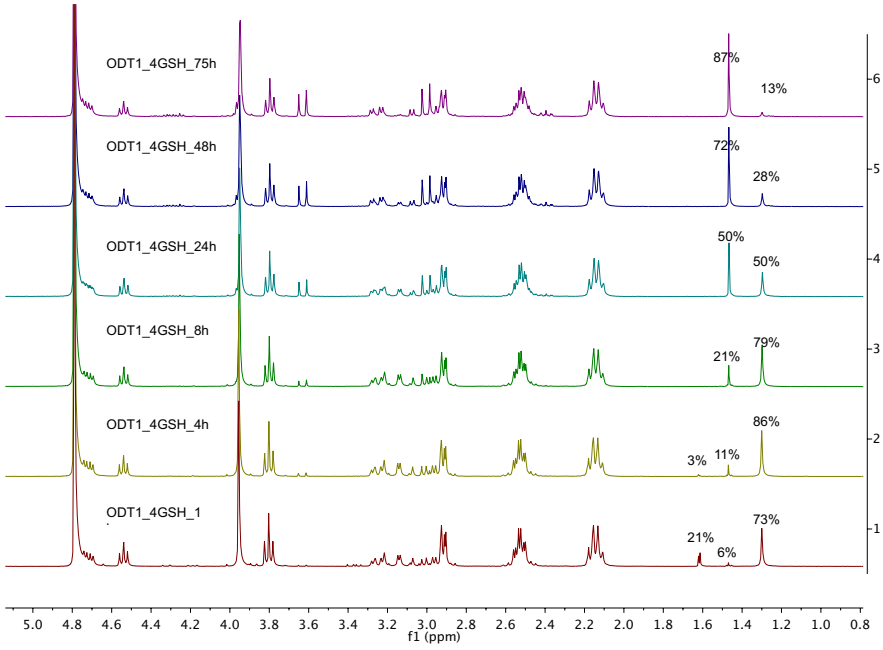

Figure A4.13. ^{1}H-NMR (400 MHz, 298K, D_2O) spectrum of the **ODT** and **GSH** mixture at specific time points with a molar ratio of thiol/ODT at 4:1

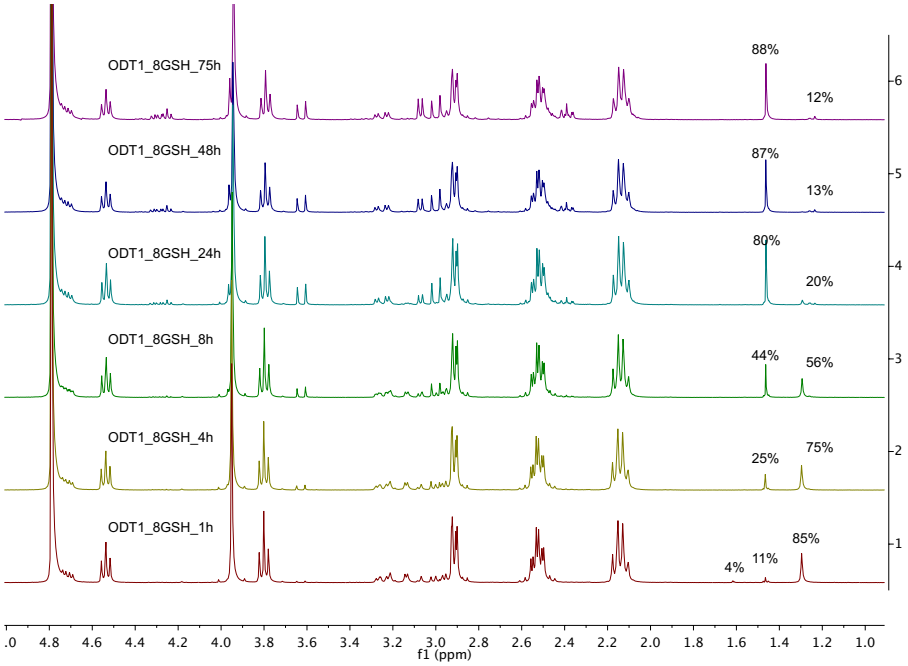

Figure A4.14. ^{1}H-NMR (400 MHz, 298K, D_2O) spectrum of the **ODT** and **GSH** mixture at specific time points with a molar ratio of thiol/ODT at 8:1

4.6.12 References

[1] X. Marat, K. Lucet-Levannier, L. Marrot, **2013**, U.S. Patent No. US8530511B2.

[2] D. P. Donnelly, M. G. Dowgiallo, J. P. Salisbury, K. C. Aluri, S. Iyengar, M. Chaudhari, M. Mathew, I. Miele, J. R. Auclair, S. A. Lopez, R. Manetsch, J. N. Agar, *J. Am. Chem. Soc.* **2018**, *140*, 7377.

[3] E. Giacomelli, M. Bellin, V. V. Orlova, C. L. Mummery, *Curr. Protoc. Hum. Genet.* **2017**, *95*, 21.9.1.